Early history of the Midcontinent Rift inferred from geochemistry and sedimentology of the Mesoproterozoic Osler Group, northwestern Ontario

Pete Hollings, Philip Fralick, and Brian Cousens

Abstract: The Mesoproterozoic 1108–1105 Ma Osler Group, a 3 km thick succession of basaltic flows and sedimentary units on the north shore of Lake Superior, is among the oldest expressions of the Midcontinent Rift. Basal sediments of the Simpson Island Formation (new name) deposited by braided fluvial systems record westward transport of debris eroded from local Archean and Proterozoic rock units. Strata deposited by this fluvial system are intercalated with, and overlain by, ocean-island basalt (OIB)-like basalts, which become increasingly contaminated up section ($\varepsilon_{Nd(1100Ma)}$ = +0.3 to –5.3). The light rare-earth element (LREE) enriched (La/Sm_n = 1.5–3.9) and heavy REE (HREE) fractionated (Gd/Yb_n = 1.5–3.7) subaerial flows are divisible into two units that correlate with other sections of the Osler Group to the east, but simple correlations with more distant sequences are difficult. The volcanic rock dominated portion of the succession is overlain by a thin (25 m thick) conglomerate–sandstone assemblage representing southeast progradation of an alluvial fan in a semi-arid climatic setting. Clast lithologies and geochemistry indicate no extra-rift detritus was delivered from the hinterland of the fan. Various lines of evidence in both volcanic and sedimentary rocks support a scenario where early, pre-1108 Ma, subsidence along a north–south axis from the western arm of the rift to the Nipigon Embayment was replaced by subsidence along the east–west rift axis between 1108 and 1105 Ma.

Résumé : Le Groupe d'Osler (Mésoprotérozoïque, 1108–1105 Ma), une succession de coulées basaltiques et d'unités sédimentaires d'une épaisseur de 3 km sur la rive nord du lac Supérieur, est l'une des plus anciennes expressions du rift mi-continental. Les sédiments à la base de la Formation Simpson Island (nouveau nom), déposés par un système fluvial anastomosé, enregistrent le transport vers l'ouest de débris érodés des unités rocheuses locales archéennes et protérozoïques. Des basaltes de points chauds recouvrent et sont intercalés avec les strates déposées par ce système fluvial; ces basaltes sont de plus en plus contaminés en remontant la section ($\varepsilon_{Nd(1100Ma)}$ = +0.3 to –5.3). Les écoulements sub-aériens de terres rares légères enrichies (La/Smn = 1,5–3,9) et de terres rares lourdes enrichies fractionnées (Gd/Ybn = 1,5–3,7) peuvent être divisés en deux unités qui correspondent à d'autres sections du Groupe d'Osler vers lst, mais de simples corrélations avec des séquences plus éloignées sont difficiles. La portion de la succession dominée par des roches volcaniques est recouverte d'un mince (25 m) assemblage conglomérat-grès qui représente la progradation vers le sud-est d'un delta alluvionnaire dans un environnement climatique semi-aride. La lithologie des clastes et la géochimie indiquent qu'aucun détritus hors du rift ne provient de l'arrière pays du delta. Diverses preuves à la fois dans les roches sédimentaires et les roches volcaniques soutiennent un scénario selon lequel une subsidence précoce (avant 1108 Ma) le long d'un axe nord–sud à partir du bras ouest du rift vers la baie Nipigon a été remplacée par de la subsidence le long de l'axe est–ouest du rift entre 1108 et 1105 Ma.

[Traduit par la Rédaction]

Introduction

A considerable amount of literature has been written on the Midcontinent Rift system detailing the petrology and geochemistry of the igneous rocks (Sutcliffe 1987; Nicholson and Shirey 1990; Lightfoot et al. 1991; Klewin and Shirey 1992; Shirey et al. 1994; Nicholson et al. 1997; Vervoort and Green 1997); the age of the igneous rocks, based on both paleomagnetic stratigraphy (Halls 1972, 1974; Palmer and Davis 1987) and radiometric dating (Hanson 1975; Van Schmus et al. 1982; Davis and Sutcliffe 1985; Krogh et al. 1987; Davis and Paces 1990; Heaman and Machado 1992; Paces and Miller 1993; Davis and Green 1997; Zartman et al. 1997; Heaman and Easton 2005); the depositional envi-

Received 6 March 2006. Accepted 17 July 2006. Published on the NRC Research Press Web site at http://cjes.nrc.ca on 3 May 2007.

Paper handled by Associate Editor W.J. Davis.

P. Hollings[1] **and P. Fralick.** Department of Geology, Lakehead University, 955 Oliver Road, Thunder Bay, ON P7B 5E1, Canada.
B. Cousens. Department of Earth Sciences, Carleton University, 1125 Colonel By Drive, Ottawa, ON K1S 5B6, Canada.

[1]Corresponding author (e-mail: peter.hollings@lakeheadu.ca).

 doi:10.1139/E06-084

ronments and dispersal systems of the sediments (Hamblin 1961; Wolff and Huber 1973; Fowler and Kuenzi 1978; Catacosinos 1981; Daniels 1982; Kalliokoski 1982; Merk and Jirsa 1982; Ojakangas and Morey 1982*a*, 1982*b*); rift architecture (Green 1983; Cannon et al. 1989; Behrendt et al. 1990; Cannon and Hinze 1992; Hinze et al. 1992; Van Schmus 1992); and the nature of the subrift lithosphere (Behrendt et al. 1990; Hinze et al. 1992). These studies have mostly dealt with the later stages of rift development. This is especially true of the seismic work, which has portrayed a fully developed rift that was later subjected to compressive forces probably generated by the Grenvillian orogeny (Cannon and Hinze 1992; Van Schmus 1992; Cannon 1994). It is now generally accepted that an upwelling mantle plume was responsible for the large volumes of mafic magmas associated with the rift (Hutchinson et al. 1990; Nicholson and Shirey 1990). The earliest history of the rift remains poorly understood, however, although scenarios have been proposed for the style of early rift development. These generally involve initial sagging without major block faulting (White 1972; Green 1977, 1981, 1983), major block faulting (Chase and Gilmer 1973; Weiblen and Morey 1980), or an early stage of sagging followed by block faulting (Cannon et al. 1989; Cannon 1992).

The oldest rift-related rocks on which U–Pb age determinations have been performed lie along the northwestern portion of the Midcontinent Rift. These include, from northeast to southwest, the alkaline intrusives of the Coldwell Complex (1108 ± 1 Ma; Heaman and Machado 1992), the lower Osler Group volcanics 1107.5^{+4}_{-2} to 1105 ± 2 Ma; Davis and Sutcliffe 1985; Davis and Green 1997), the Logan Sills (1109^{+4}_{-2} Ma; Davis and Sutcliffe 1985), the lower portion of the North Shore Volcanics (1108 ± 2 Ma; Davis and Green 1997), the Swamper Lake Gabbro and Nathan's Series intrusive rocks (1107 Ma; Paces and Miller 1993), and the lower portion of the Powder Mill Group (1107 ± 2 Ma; Davis and Green 1997). Recent work dating the mafic–ultramafic intrusions in the vicinity of Lake Nipigon has yielded an age of 1124 Ma for the Seagull intrusion, and the extensive diabase sills range in age from 1109 to 1113 Ma (Heaman and Easton 2005). These older units crop out on the rift flanks where erosion has removed the younger rift sequence or, in the case of the Coldwell and diabase sills, are intruded into older rocks immediately north of the rift. Of the units listed previously, the excellent outcrops of the lower volcanic and sedimentary units in the Osler Group provide the best opportunity for acquiring data that could illuminate the processes involved in the earliest stage of the Midcontinent Rift system.

The volcanic and sedimentary units of the Osler Group were studied on the islands adjacent to Nipigon Bay, northern Lake Superior (Fig. 1), and data from there plus major, trace, and isotopic analyses are combined to ascertain the dynamics of early rift development in this segment of the basin. Not only can the geochemical stratigraphy of the volcanics and its causative factors be derived from this sequence, but also the sedimentary units furnish information on the paleogeography at the time of extrusion and, by extension, the style of subsidence. Together these have the capacity to provide the most detailed picture of the early rift to date.

Local geology

Basal sedimentary strata of the Osler Group rest with angular unconformity on eolian and lacustrine deposits of the <1450 Ma Sibley Group (Figs. 1C, 2). In addition to the erosional disconformity evident in outcrop, regional mapping has shown that the Sibley Group was tilted west side down and erosively leveled prior to deposition of the Osler Group (Rogala et al. 2005). The Sibley Group itself rests with erosional disconformity on the Paleoproterozoic Gunflint Formation of the Animikie Group (Figs. 1C, 2).

Neoarchean igneous and sedimentary rocks, which were metamorphosed during the 2.7 Ga Kenoran orogeny, crop out at the surface north of the study area (Fig. 1C). In the vicinity of Lake Nipigon, these Neoarchean rocks and the overlying strata of the Animikie and Sibley groups were intruded by the earliest phase of rift activity recognized to date. Here, 1124–1109 Ma mafic–ultramafic intrusions and up to 300 m thick, 1113–1109 Ma mafic sills herald the beginning of igneous activity associated with the rift (Heaman and Easton 2005). The lower Osler Group volcanic rocks are slightly younger (~1 million years) than the majority of the diabase sills in the Lake Nipigon area.

The lowermost 100 m of the Osler Group contains abundant sandstones and conglomerates that form its base and intercalate with the lowest basalt flows (Fig. 2). Above this zone, interflow sediments are typically thin and of limited extent. The exception to this is the Puff Island conglomerate (Fig. 2), a 25 m thick sedimentary unit that lies ~2700 m above the base of the Osler Group and marks a paleomagnetic reversal. The majority of the exposed basalt-dominated section is magnetically reversed, with only the upper 100 m displaying a normal polarity (Halls 1974). The contact between the two units of contrasting magnetic polarity is marked by the presence of the Puff Island conglomerate and a discordance between the basalt flows above and below the contact (Fig. 2). This has been interpreted as representing a significant break in the eruption history (Halls 1974). A felsic porphyry immediately above the sedimentary rocks at the base of the Osler Group yielded a U–Pb zircon age of 1107.5^{+4}_{-2} Ma (Davis and Sutcliffe 1985), whereas zircons from the Agate Point rhyolite towards the top of the reversely magnetized basaltic rocks yielded an age of 1105 ± 2 Ma (Fig. 2) (Davis and Green 1997). Based on interpretation of deep seismic reflection profiles through the Osler Group ~90 km to the southeast, under Lake Superior, Cannon et al. (1989) have proposed that the total thickness of the group is ~3 km.

Description of sedimentary and volcanic units

The sedimentary successions near the base of the Osler Group constitute the Simpson Island Formation (new name, see Fig. 3 for location of the composite stratotype, lithologies, and contact relationships; Appendix A). The Simpson Island Formation is composed of a lower member dominated by trough cross-stratified, medium-grained sandstones directly overlying basement and an upper member with a greater variety of siliciclastic units (Figs. 2, 3). The two members are

Fig. 1. (A) Map of upper Great Lakes showing the location of the study area. (B) Regional geology map showing the extent of the exposed portion of the Osler Group. Age data from Davis and Sutcliffe (1985) and Davis and Green (1997). Modified after Sutcliffe (1987). (C) Geological map of the Osler Group showing sample locations. The prefix OV indicates volcanic rocks of the Osler Group, and the prefix OS indicates sedimentary rocks. Modified after Giguère (1975).

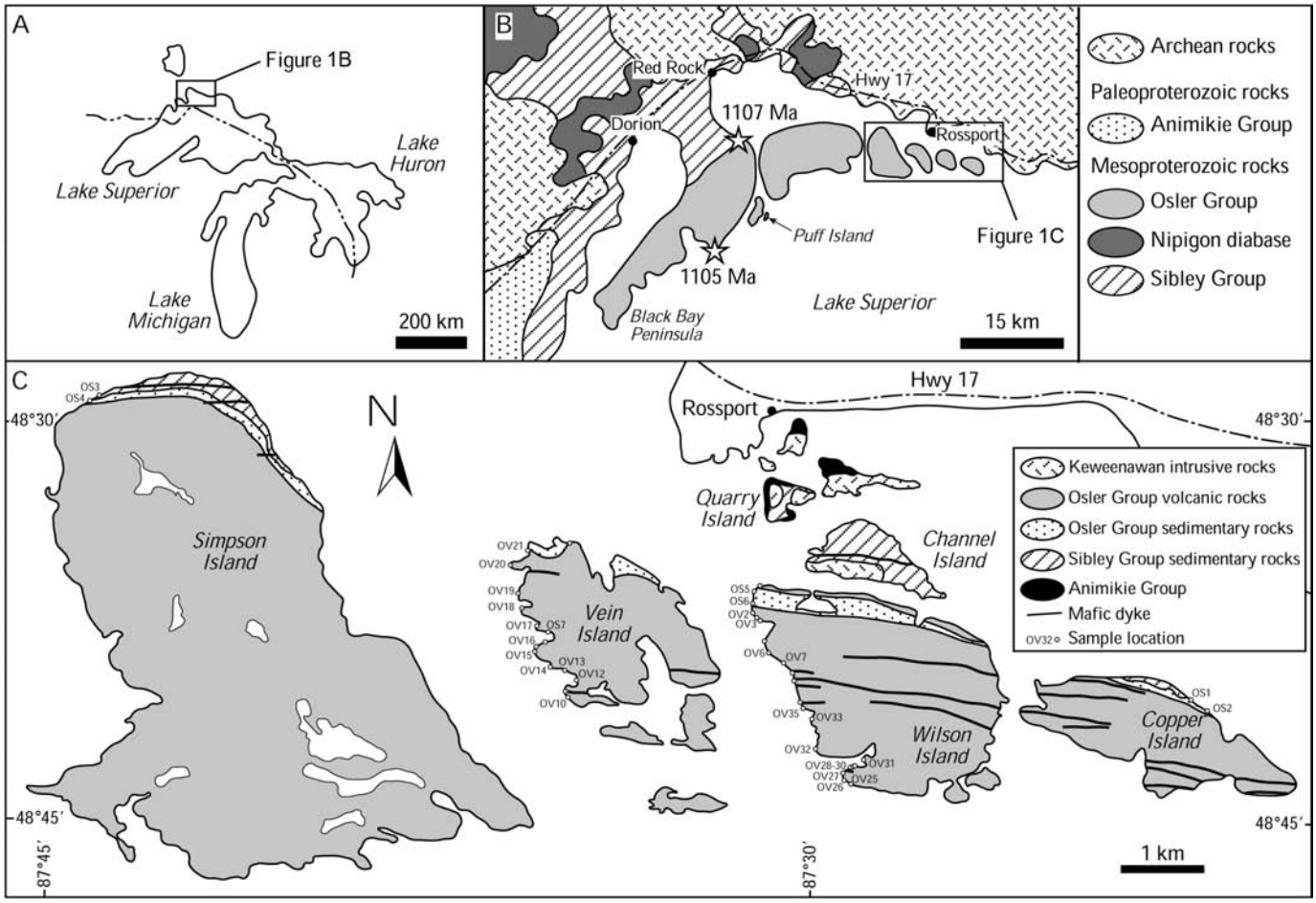

separated by 10–50 m of mafic and felsic volcanic rocks, which are considered to represent an interfingering contact between the Simpson Island Formation and the overlying unit of similar basalts. The lower member sits on an irregular, erosional surface cut into the underlying quartz arenites and red shales of the Sibley Group. A massive pebble–cobble conglomerate overlies the unconformable surface and is in turn overlain by decimetre-scale layers of coarse-grained and pebbly sandstone (Fig. 3, section 1). Sandstones are parallel laminated and commonly have cross-stratified tops. More rarely they contain pebbly transverse ribs (cf. McDonald and Banerjee 1971; Boothroyd and Ashley 1975) and chute- and pool-like structures (cf. Fralick 1999). Thin limestones, rich in siliciclastic sand, are developed in places. The central portion of the lower member is composed of trough cross-stratified, medium-grained sandstone organized into a stacked assemblage of lenses. Pebble stringers and pebbly sandstones commonly occur on the deeper portions of curving set boundaries (Fig. 3, section 2). Massive pebble–cobble conglomerates sharply overlie the sandstone succession (Fig. 3, sections 2 and 4). The conglomerates contain trough cross-stratified, medium-grained sandstone lenses. Decimetre- to metre-scale wedges of planar cross-stratified sandstone are interbedded with assemblages of trough cross-stratified sandstones up to 1 m thick. Another assemblage of trough cross-stratified sandstone, similar to that in the central portion of the succession, caps the lower member of the Simpson Island Formation (Fig. 3, sections 3 and 4). Clasts in the pebble–cobble population are dominated by quartz, chert, various types of volcanic rocks, red siltstone, metamorphosed granite, and at the east end of the outcrop belt, on Copper Island, a higher proportion of unmetamorphosed red granite. Paleocurrent indicators show flow was to the west, averaging 265° (Fig. 3).

The basal sedimentary rocks of the lower member are overlain on eastern Simpson Island by a quartz–feldspar porphyry, which appears to be a flow with a U–Pb age of 1107.5 Ma (Davis and Sutcliffe 1985). Basalt lies to the east and west of this limited area. Another sedimentary assemblage is present on Vein Island (Fig. 3, section 5) separated from the lower member by a few tens of metres of basalt (Fig. 2). Basal sandstones and conglomerates of this portion of the upper member of the Simpson Island Formation are organized into sharp-sided, decimetre-thick, parallel-laminated, laterally continuous beds. Some are poorly sorted with chaotic clast orientations. The upper portion of this section

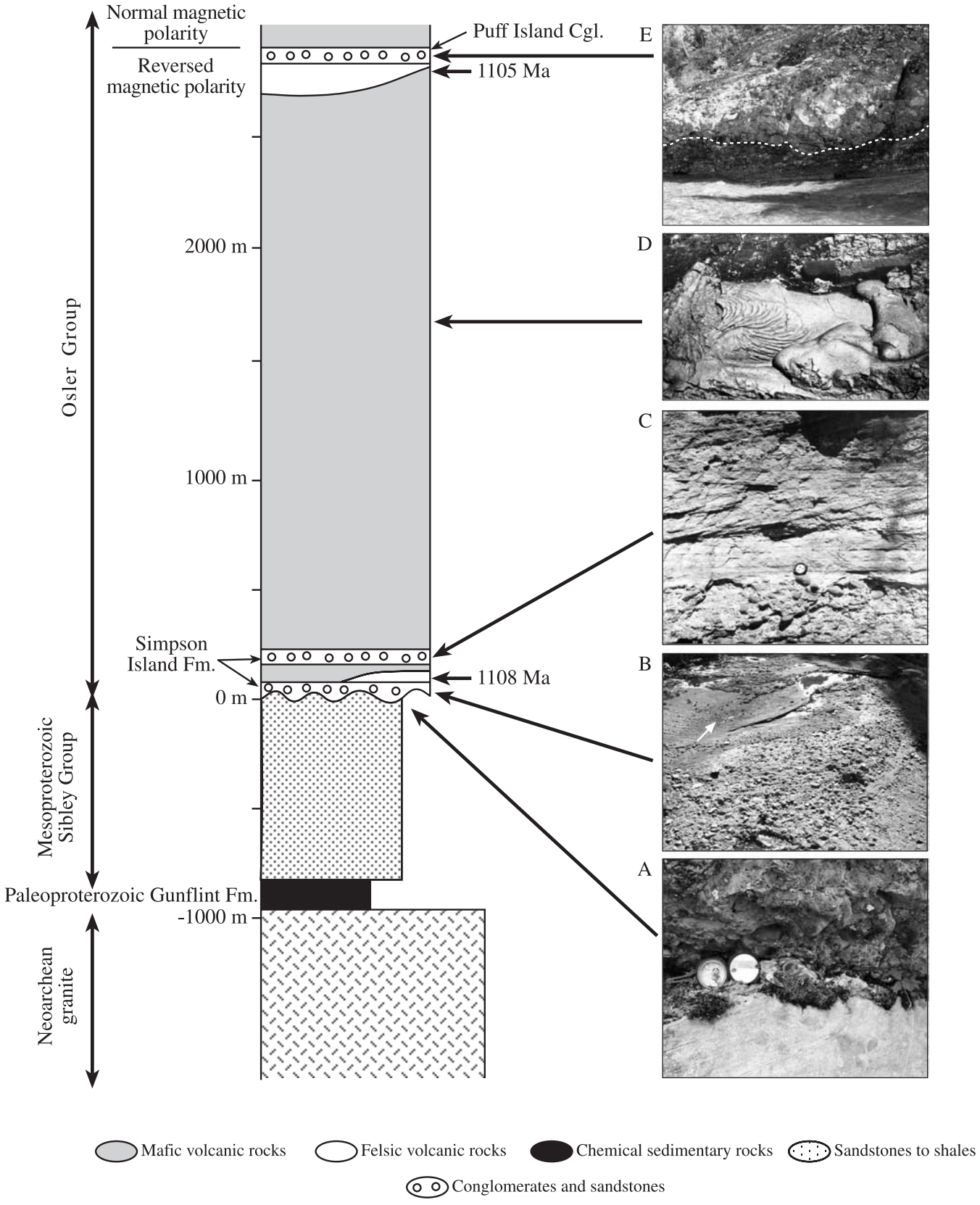

is composed of cobble–pebble conglomerates with trough cross-stratified sandstone lenses and more laterally continuous, elongate wedges of sandstone. Some wave-oscillation ripples are present. Clasts are dominated by quartz arenites from the Sibley Group, with minor basalt and granite fragments. Paleocurrents are to the west, averaging 268°.

Fig. 2. Generalized stratigraphy of the Osler Group and underlying units. The Simpson Island Formation of the basal Osler Group rests with angular unconformity on the underlying Sibley Group. The upper contact of the Osler Group is covered by Lake Superior. The lower member of the Simpson Island Formation is the sedimentary unit at the base of the Osler Group. The upper member is located near the base of the group overlying intercalated basalt. The Puff Island sedimentary rocks are at the top of the Osler Group. Photographs of the units are from the bottom (A) to the top (E) of the succession as follows. (A) Unconformity between the underlying eolian sandstones of the Sibley Group (below the compass) and the lower member of the Simpson Island Formation, Osler Group (Fig. 3, section 1). (B) Conglomerates forming a longitudinal bar with a broad chute channel filled with cross-stratified sandstone, lower member, Simpson Island Formation (Fig. 3, section 4; arrow denotes paleocurrent direction; compass centre left for scale). (C) Conglomerate overlain by parallel-laminated and trough cross-stratified channel sandstone, upper member, Simpson Island Formation (Fig. 3, section 6; compass for scale). (D) Pahoehoe flow within the Osler Group on Wilson Island (glasses case for scale). (E) Parallel-bedded sheetflood deposits (below broken line) overlain by a mass flow with clasts up to 1 m diameter. The layered conglomerate and sandstone at the top of the hill represent small, stacked channels, Puff Island assemblage (Fig. 3, section 7). The field of view is 4 m across. Fm., Formation; Cgl, conglomerates.

Another sedimentary assemblage of the upper member occurs on Wilson Island (Fig. 1), overlying ~50 m of basalt that separates it from the lower member. This upwards-coarsening succession has oscillation-rippled, very fine-grained sandstones at its base. These coarsen upwards by the addition of increasing amounts of medium-grained, parallel-laminated to hummocky cross-stratified to oscillation-rippled, decimetre-scale sandstone beds. A covered interval separates this assemblage from overlying medium- to large-scale, trough cross-stratified, coarse-grained sandstones to conglomerates. Paleocurrent indicators show flow to the west, though with a higher variance than that of other sections (Fig. 3). Clast lithologies are similar to those in the lower member.

A sedimentary assemblage, the Puff Island conglomerate, also occurs near the upper stratigraphic limit of outcrop of the Osler Formation, at the top of the magnetically reversed interval (Figs. 1–3, section 7). These interflow sediments are located on Puff Island and overlie a sequence of flow-banded rhyolites, with a U–Pb age of 1105 Ma (Davis and Green 1997). They contain assemblages of sharp-sided, laterally continuous, pebbly, coarse-grained sandstone beds with caliche horizons, which are scoured into by small lenses of conglomerate; large scours filled with trough cross-sets more than 1 m thick; stacked assemblages of irregular lenses filled by trough cross-stratified, coarse-grained, pebbly sandstone; and poorly sorted, disorganized, massive boulder–cobble conglomerate. Clasts are all volcanic, ranging in composition from quartz–feldspar porphyry to basalt. Paleocurrents on large-scale sedimentary structures consistently show flow was to the southeast.

Quartz–feldspar porphyry and basalt separate the Simpson Island Formation into its two informal members. These basalts are geochemically similar to the overlying basalts and are thus viewed as an intercalation of the thick basaltic pile with the Simpson Island Formation. The mafic strata of the Osler Group consist of massive to amygdaloidal flows, with locally developed ropey tops and pahoehoe textures (Fig. 2) (Sutcliffe and Smith 1988). The flows range in thickness from 5 cm to 30 m (Lightfoot et al. 1991), with a regional dip of ~6°S–15°S (Giguère 1975; Lightfoot et al. 1991; this study). All flows sampled in this study come from the reversed-polarity portion of the section below the Puff Island conglomerate (Fig. 2). Detailed descriptions of the Osler Group are provided by McIlwaine and Wallace (1976) and Lightfoot et al. (1991). Flows sampled for geochemical analysis were typically >1 m thick, were amygdaloidal towards the top and bottom of the flow, and have a massive core, with the samples themselves being taken from the cores of the flows. They rarely display a pahoehoe texture on the flow surface (Fig. 3). In places, the mafic flows preserve vesicle columns up to 10 cm in diameter. These typically occur above thin sequences of interflow sediments, suggesting they formed as a result of the passage of the flow over the wet sediment. The interflow sediments generally occur as thin, flow-parallel units but in places have infilled vertical cooling cracks within the flows. The basalts are characterized by clinopyroxene and plagioclase phenocrysts in a groundmass of plagioclase, augite, and Fe–Ti oxides. Rarely, basalts from the base of the sequence contain pseudomorphed olivine phenocrysts now preserved as amphibole. The basalts have all been subjected to metamorphism ranging from zeolite to prehnite–pumpellyite facies (McIlwaine and Wallace 1976).

Geochemistry

Twenty-five samples of mafic volcanic rock were collected vertically through the stratigraphy on two transects, one on Vein Island and one on Wilson Island (Fig. 1C). The samples were analyzed for major and trace elements, with a subset of nine samples selected for radiogenic isotope analysis. Major elements were determined for the mafic igneous rocks by X-ray fluorescence spectrometry (XRF), and trace elements, including the rare-earth elements (REE) and high field strength elements (HFSE), were analyzed using inductively coupled mass spectrometry (ICP–MS; Table 1) at the Department of Geological Sciences, University of Saskatchewan, Saskatoon, Saskatchewan. In addition, nine samples of medium-grained sandstone were collected from the sedimentary units (Table 2) and analyzed at the Ontario Geological Survey laboratories in Sudbury, Ontario.

The volcanic rocks are all basalts or basaltic andesites (SiO_2 = 47–56 wt.%; MgO = 5–16 wt.%; Table 1), similar to the range of lava compositions reported from a previous study of the Osler Group and from the Mamainse Point section (Lightfoot et al. 1991; Shirey et al. 1994). In Harker variation diagrams, the Osler basalts show trends of decreasing MgO, TiO_2, and Fe_2O_3 but increasing Th with increasing SiO_2 (Fig. 4). When major and trace element data are evaluated with relation to their stratigraphic position (Fig. 5), it can be seen that there is a broadly increasing SiO_2 and decreasing MgO with an increase in height above the Simpson Island Formation. The basalts are characterized by light REE

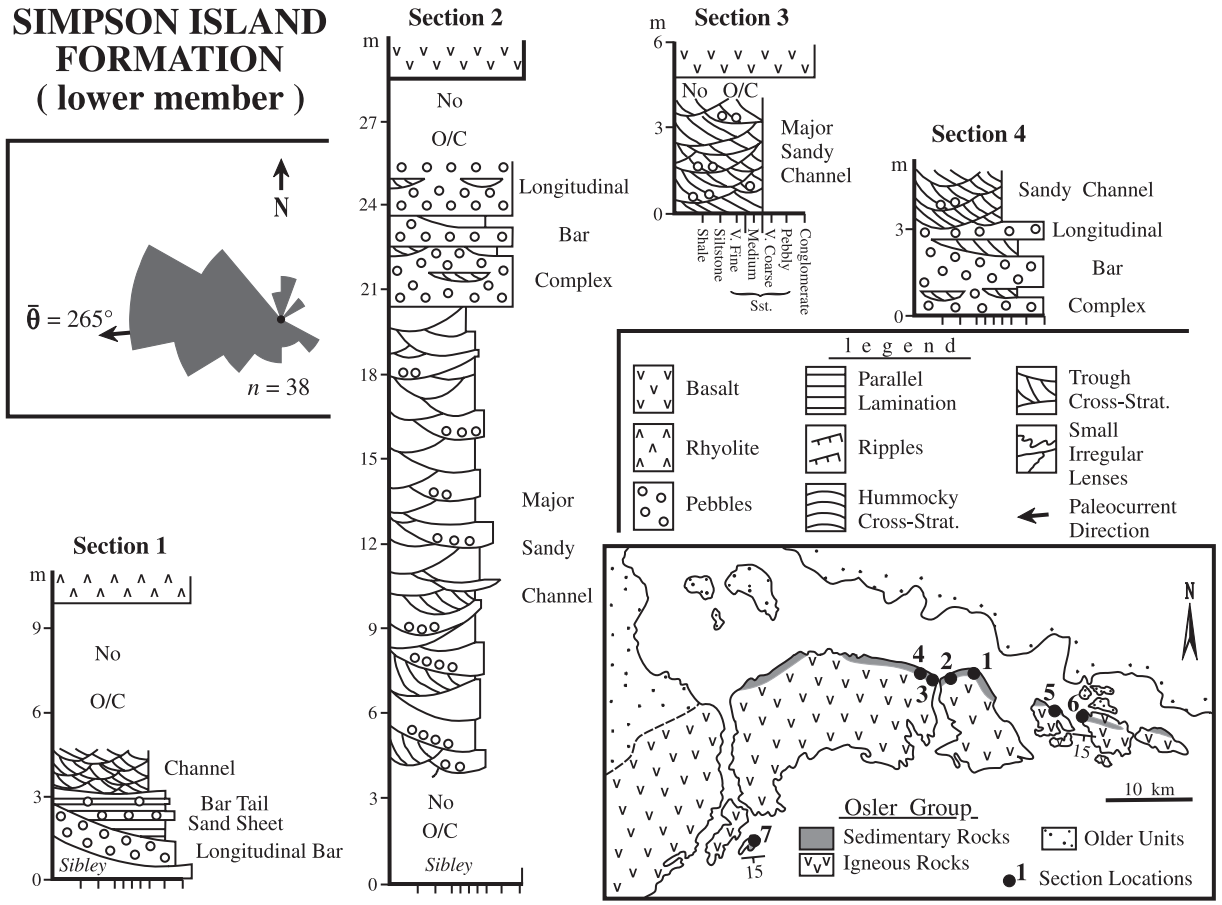

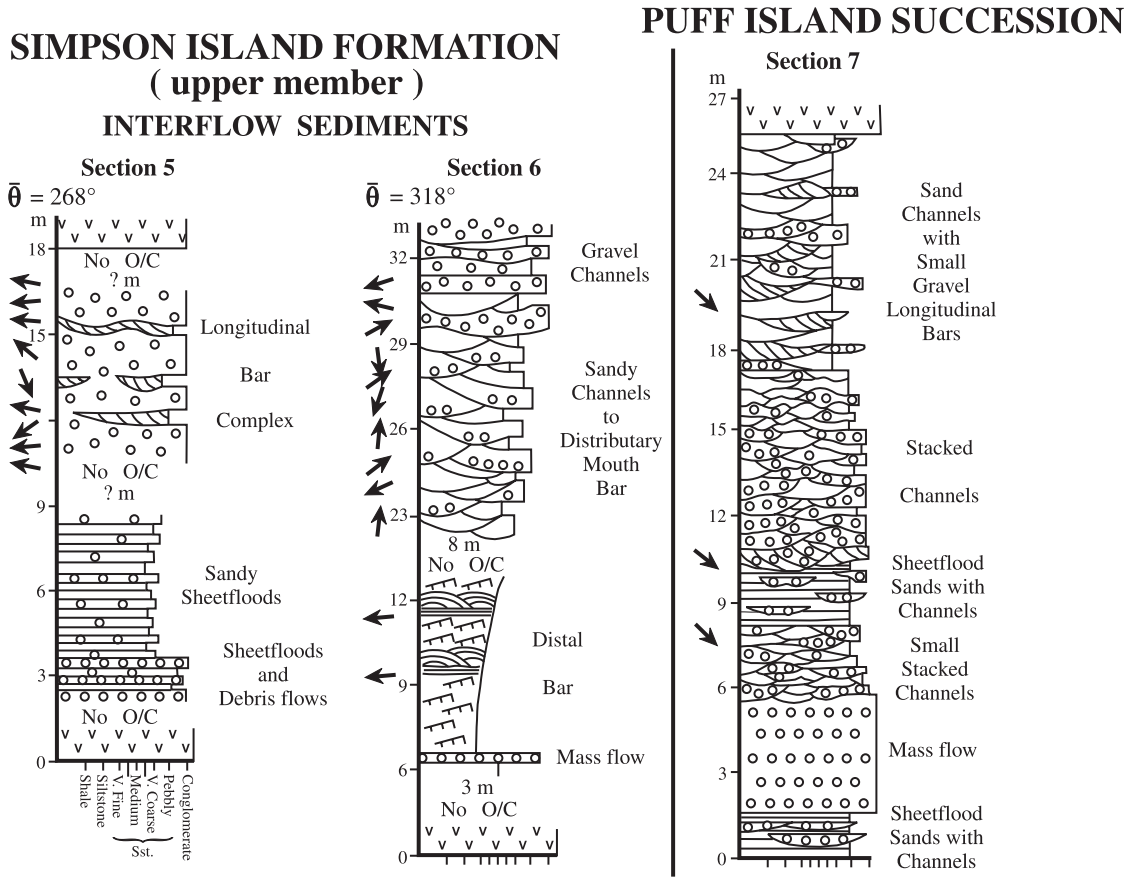

Fig. 3. Stratigraphic sections of sedimentary rocks in the Osler Group. Sections 1–4 are the basal sedimentary succession of the Osler Group forming the lower member of the Simpson Island Formation at different locations (see inset map). These represent the composite stratotype of the lower portion of this formation. Sections 5 and 6 are of the upper member, Simpson Island Formation. These represent the composite stratotype of the upper member of the Simpson Island Formation. The lower member (section 5) and section 6 are all separated by interfingering basalt flows. Section 7 is the sedimentary assemblage near the top of the Osler Group on Puff Island. Paleocurrent measurements ($\bar{\theta}$) were corrected for the dip of the bedding and indicate flow to the west for the Simpson Island Formation and flow to the southwest for the Puff Island assemblage. O/C, outcrop; Sst., sandstone; Strat., stratified.

(LREE) enrichment (La/Sm_n = 1.5–3.9) in conjunction with moderately fractionated heavy REE (HREE; Gd/Yb_n = 1.5–3.7) and slight positive to moderately negative Nb anomalies (Nb/Nb* = 0.56–1.13; Fig. 6). Up section, the basalts display strong positive correlations between La/Sm_n, Th/La, and Th/Nb (Fig. 5). This correlation is most pronounced above 400 m, with samples from the base of the stratigraphy displaying more or less constant values of these ratios (Fig. 5). Measured $^{143}Nd/^{144}Nd$ ratios for the seven Osler basalts analyzed range from 0.511857 to 0.512286 with $\varepsilon_{Nd(t = 1100\ Ma)}$ of +0.3 to –5.3 and $^{87}Sr/^{86}Sr$ of 0.704039–0.709219 (Table 3). As with the major and trace element data, the radiogenic isotope data display strong correlations with height above the contact, with a trend to decreasing $^{143}Nd/^{144}Nd$ but increasing $^{87}Sr/^{86}Sr$ (Table 3).

Medium-grained sandstones were sampled to gain further information on the provenance of the sedimentary units of the Simpson Island Formation. The sandstones of this succession are predominantly lithic arkoses with angular to subrounded grains and abundant fine-grained matrix. Sample locations are given in Fig. 1C. In addition, two samples were collected from the stratigraphically highest sedimentary unit, the sandstones and conglomerates on Puff Island (Figs. 1B, 2, 3). The geochemistry of the nine sandstone samples is not necessarily representative of all the sedimentary rocks in the stratigraphic section but does reflect the composition of the discrete layers from which they were taken (Table 2). These data can be used to constrain the provenance of these layers. If two chemically immobile elements, which are contained in major mineral phases that behaved in hydrodynamically similar manners during transport, are expressed as a ratio, it will reflect the weighted average ratio of the source material of these samples (Fralick and Kronberg 1997; Fralick 2003). By comparing similar ratios for samples at differing stratigraphic positions, insight can be gained into the evolutionary trend of the provenance.

The geochemistry of sandstone samples indicates that three general trends occur. The three stratigraphically highest samples are enriched in the first-row transition metals. The uppermost sample in the lower member of the Simpson Island Formation and, to a greater extent, the lower sample in the upper member are enriched in HFSEs, and the remaining four samples of the Simpson Island Formation have relatively low values of most trace elements (Fig. 7). The division of the samples according to these three general trends is equivocal, as overlap occurs. For example, the interflow sediment sample (third from top, Fig. 7) is enriched in both first row transition metals and HFSEs.

Discussion

Geochemistry

The most primitive basalts analyzed in this study, with the highest MgO, Cr, and Ni, are located towards the base of the stratigraphic succession (Fig. 5). The elevated MgO and Cr contents suggest that sample OV-21, which lies directly above the Simpson Island Formation, is likely the most primitive basalt and consequently represents the closest to primary magma compositions. Unlike the Mamainse Point Formation, no picrites are present at the base of the Osler volcanic sequence. The high incompatible element abundances, in conjunction with LREE enrichment and strongly fractionated HREE, are comparable to modern ocean-island basalts (OIB), albeit at lower absolute abundances (Fig. 8A). When compared to other flood basalt sequences, the more primitive basalts, forming the lower sequence of mafic rocks in the Osler Group, closely resemble basalts from the Parana–Etendeka sequence (Fig. 8A; Gibson et al. 2000). White and McKenzie (1995) calculated, based on inversion of REE data from this "lower suite" in the Osler Group, that the initial magma type represented small-degree partial melts that last equilibrated with a garnet-bearing residue, and this is consistent with our data. Nicholson and Shirey (1990) suggested that the main volume of rift basalt was produced from an enriched mantle plume with an ε_{Nd} value close to zero and chondrite-normalized La/Sm of 2–3, which is consistent with isotopic and trace element data from many basalt sequences in the rift (Fig. 9A) (Paces 1988; Nicholson et al. 1991; Wirth et al. 1997). Depleted mantle at 1100 Ma would have had a positive ε_{Nd} perhaps as high as +6, whereas an enriched plume source would have ε_{Nd} less than that of depleted mantle (Nicholson and Shirey 1990; Shirey et al. 1994). The low ε_{Nd} and lack of Nb depletion relative to La or Th from the most primitive members of the Osler Group are consistent with a mantle plume rather than a crustally contaminated depleted mantle source.

High MgO, Ni, and Cr contents in samples from near the base of the Osler Group are consistent with them being the most primitive end members. Basalts lower in the stratigraphic succession also have ε_{Nd} of around zero. Up sequence, the basalts are characterized by lower MgO, Ni, and Cr but higher SiO_2, Th, and La/Sm_n abundances in conjunction with increasingly negative Nb and Ti anomalies and $\varepsilon_{Nd(1100\ Ma)}$ values of –4 to –5. This trend is consistent with contamination of this upper sequence of basalts by an older lithospheric component characterized by pronounced LREE enrichment and high Th abundances but generally unfracti-

Table 1. Major and trace element data for the Osler Group volcanic rocks.

	OV-2	OV-3	OV-6	OV-7	OV-35	OV-33	OV-32	OV-31	OV-28	OV-29
SiO_2 (wt.%)	51.46	49.91	48.04	48.89	50.29	52.79	52.47	55.59	53.10	53.42
TiO_2	2.54	2.18	1.82	2.65	1.88	1.30	1.16	1.07	1.02	1.09
Al_2O_3	11.72	10.32	15.78	10.47	10.21	14.28	15.31	13.76	14.87	14.69
Fe_2O_3	13.73	15.93	14.16	15.63	14.38	12.06	11.46	11.62	11.16	11.28
MnO	0.10	0.15	0.19	0.18	0.17	0.16	0.17	0.14	0.17	0.18
MgO	9.07	9.20	6.70	8.19	11.37	5.55	5.83	5.69	5.97	5.58
CaO	9.02	9.56	10.19	10.94	8.90	10.28	10.15	8.14	9.43	9.86
K_2O	1.89	2.00	2.54	2.17	1.93	2.44	2.48	2.80	2.82	2.74
Na_2O	0.24	0.53	0.38	0.62	0.69	0.98	0.81	1.03	1.30	0.99
P_2O_5	0.23	0.20	0.20	0.25	0.18	0.16	0.16	0.15	0.15	0.16
Mg#	0.59	0.56	0.51	0.54	0.64	0.50	0.53	0.52	0.54	0.52
Sum	99.77	99.48	99.59	99.38	99.90	100.30	99.69	100.30	99.90	100.50
LOI	4.20	1.50	0.20	0.45	1.20	0.95	0.95	1.45	1.00	0.75
Ti (ppm)	15 145	12 965	10 873	15 778	11 226	7 807	6 900	6 448	6 116	6 584
P	1 002	886	875	1 096	795	705	705	664	661	703
Cr	1 045	767	266	868	1 026	170	143	130	89	96
Co	88	69	98	95	84	50	50	43	51	49
Ni	305	248	243	230	405					
Rb	3.69	8.59	3.62	12.73	14.63	18.67	8.71	7.73	31.51	23.25
Sr	471	414	315	470	307	363	393	328	350	324
Cs	0.11	0.15	0.15	0.10	0.22	0.09	0.00	0.16	0.34	0.19
Ba	354	304	163	203	315	438	414	549	582	425
Sc	35.77	45.54	42.90	45.28	33.49	42.62	52.10	50.87	39.52	39.56
V	403	346	291	428	337	329	291	231	259	292
Ta	0.87	0.61	0.55	0.92	0.65	0.92	1.12	1.15	1.33	1.45
Nb	20.23	13.14	10.10	18.92	12.91	18.62	19.92	18.46	26.41	30.15
Zr	242	163	125	233	179	141	133	115	169	191
Hf	4.69	4.53	3.68	5.62	4.45	3.02	3.24	3.09	3.73	3.93
Th	1.66	1.34	0.98	1.63	2.94	3.35	2.97	2.81	4.17	4.79
U	0.41	0.29	0.19	0.38	0.44	0.77	0.72	0.58	0.93	1.14
Y	26.44	20.62	25.91	28.67	27.05	25.32	22.28	19.88	24.33	26.79
La	20.94	17.25	12.57	21.70	19.37	20.40	20.93	20.11	25.92	27.86
Ce	50.59	41.84	29.45	53.97	43.52	42.07	43.07	41.19	52.86	58.08
Pr	6.95	6.00	4.14	7.26	5.88	5.19	5.31	4.81	6.15	6.61
Nd	29.64	25.59	17.15	31.95	22.92	20.14	19.45	19.06	22.66	25.61
Sm	6.84	5.83	4.83	7.82	5.82	4.31	4.17	3.89	4.31	4.85
Eu	2.30	1.97	1.77	2.43	1.76	1.43	1.41	1.34	1.44	1.60
Gd	6.35	5.97	5.17	7.32	6.01	4.32	4.56	4.04	4.60	5.16
Tb	0.83	0.79	0.76	0.99	0.88	0.69	0.66	0.55	0.63	0.69
Dy	4.58	4.44	4.96	5.40	5.05	4.23	4.01	3.73	4.10	4.55
Ho	0.75	0.81	0.93	0.99	0.99	0.90	0.80	0.76	0.86	0.89
Er	2.13	1.98	2.70	2.60	2.57	2.31	2.26	2.08	2.43	2.37
Tm	0.25	0.26	0.38	0.34	0.34	0.36	0.32	0.30	0.31	0.38
Yb	1.42	1.51	2.59	2.11	2.20	2.26	2.11	1.95	2.13	2.29
Lu	0.20	0.22	0.34	0.24	0.33	0.31	0.30	0.28	0.32	0.33
La/Yb_n	10.60	8.17	3.48	7.39	6.32	6.48	7.10	7.40	8.71	8.71
La/Sm_n	1.98	1.91	1.68	1.79	2.15	3.06	3.24	3.34	3.89	3.71
Gd/Yb_n	3.71	3.26	1.65	2.88	2.26	1.58	1.79	1.71	1.78	1.86
Al_2O_3/TiO_2	4.62	4.74	8.66	3.95	5.44	10.98	13.25	12.82	14.54	13.42
Th/Nb	0.08	0.10	0.10	0.09	0.23	0.18	0.15	0.15	0.16	0.16
Th/La	0.08	0.08	0.08	0.08	0.15	0.16	0.14	0.14	0.16	0.17
Zr/Y	9.15	7.90	4.83	8.12	6.61	5.57	5.97	5.77	6.93	7.12
Nb/Nb	0.87	0.69	0.70	0.81	0.56	0.70	0.73	0.70	0.77	0.84
Easting	461500	461550	461800	462150	462851	462838	462852	464000	463652	463652
Northing	5404350	5404200	5403450	5403200	5402304	5401902	5401438	5400950	5400873	5400873
Height (m)	133	159	290	333	489	558	639	724	737	737

Table 1 (*continued*).

OV-30	OV-27	OV-26	OV-25	OV-21	OV-20	OV-19	OV-18	OV-17	OV-15	OV-16
48.08	53.40	52.52	51.58	46.50	47.94	49.15	47.42	49.78	51.26	52.00
1.73	1.02	0.98	1.00	2.82	1.76	2.80	2.47	1.84	1.09	1.32
16.99	14.56	15.34	15.80	7.63	15.77	10.57	11.93	10.50	15.94	14.30
13.51	11.41	10.94	11.11	15.82	13.84	15.16	15.78	14.06	10.87	12.17
0.20	0.19	0.16	0.15	0.28	0.19	0.21	0.18	0.19	0.20	0.20
6.22	6.02	6.51	6.55	15.97	7.37	8.53	8.73	11.61	6.65	6.16
10.13	8.21	9.18	8.17	9.53	9.98	8.92	10.46	9.09	10.61	10.22
2.54	3.23	2.92	3.97	1.07	2.57	3.62	2.16	1.51	2.44	2.57
0.42	1.81	1.31	1.53	0.15	0.40	0.74	0.63	1.25	0.79	0.90
0.18	0.15	0.14	0.13	0.23	0.19	0.31	0.23	0.16	0.13	0.16
0.50	0.54	0.57	0.56	0.69	0.54	0.55	0.55	0.65	0.57	0.53
100.00	100.60	100.40	100.70	98.89	100.20	99.24	99.54	99.50	100.20	99.64
1.30	1.35	1.15	2.50	3.30	0.03	1.80	1.35	1.55	1.35	0.70
10 386	6 137	5 883	6 025	16 683	10 554	16 608	14 707	10 962	6 563	7 849
796	664	618	582	993	829	1 333	1 018	709	575	703
217	86	103	91	2 007	208	757	616	813	143	168
69	50	52	49	108	70	103	91	87	46	54
153		59	63	926	165	306	275	375	87	
9.09	54.77	13.54	8.44	4.07	8.40	7.95	5.50	7.45	14.61	13.35
353	361	405	746	374	324	258	357	400	358	337
0.20	1.63	0.34	0.11	1.59	0.37	0.03		0.06	0.20	0.05
141	612	378	393	84	166	190	223	251	312	393
39.43	33.71	44.37	44.99	39.04	36.26	48.03	41.35	38.84	42.90	46.62
330	238	226	200	401	291	365	390	290	235	346
0.49	1.26	1.12	1.17	1.01	0.52	0.90	0.63	0.49	0.70	0.84
10.32	22.71	19.48	19.98	19.90	10.54	16.35	12.16	9.42	12.81	17.78
110	143	127	137	219	123	223	170	130	99	134
3.04	3.51	3.45	3.99	5.41	3.26	6.52	5.15	3.83	2.76	3.10
1.14	4.42	3.33	3.61	1.31	0.95	1.81	1.43	1.63	2.27	3.18
0.32	1.05	0.61	0.72	0.41	0.25	0.00	0.31	0.29	0.55	0.66
26.67	21.32	21.32	22.68	25.44	25.26	26.97	23.06	18.76	18.78	24.90
10.62	25.59	21.75	22.21	17.31	11.93	23.05	17.84	14.45	15.54	19.21
25.73	52.88	44.38	46.43	45.65	28.53	60.29	44.35	35.09	32.26	41.16
3.46	6.10	5.16	5.41	6.67	3.86	8.32	5.84	4.59	3.99	5.10
15.80	22.76	19.03	20.12	29.70	17.09	37.45	27.72	20.01	15.32	19.92
3.82	4.57	3.93	4.22	7.52	4.08	8.50	5.88	4.65	3.50	3.93
1.46	1.54	1.26	1.28	2.22	1.46	2.48	2.07	1.49	1.20	1.42
4.36	4.91	4.24	3.93	7.03	4.62	8.25	6.25	4.64	4.12	4.26
0.68	0.65	0.59	0.61	0.98	0.71	1.03	0.84	0.62	0.54	0.68
4.26	4.13	3.86	3.81	5.14	4.26	6.14	4.94	3.83	3.25	3.95
0.88	0.82	0.72	0.74	0.94	0.90	1.04	0.85	0.71	0.67	0.89
2.46	2.48	2.10	2.14	2.32	2.52	2.71	2.37	1.74	1.93	2.29
0.36	0.33	0.31	0.33	0.27	0.36	0.32	0.28	0.23	0.28	0.34
2.28	2.16	2.05	2.12	1.66	2.17	1.92	1.72	1.49	1.72	2.22
0.34	0.31	0.28	0.31	0.21	0.33	0.27	0.23	0.20	0.27	0.32
3.35	8.50	7.60	7.52	7.46	3.95	8.62	7.43	6.97	6.48	6.21
1.80	3.62	3.57	3.40	1.49	1.89	1.75	1.96	2.01	2.87	3.15
1.59	1.88	1.71	1.54	3.50	1.76	3.56	3.00	2.58	1.98	1.59
9.80	14.30	15.68	15.81	2.70	8.97	3.78	4.83	5.70	14.57	10.87
0.11	0.19	0.17	0.18	0.07	0.09	0.11	0.12	0.17	0.18	0.18
0.11	0.17	0.15	0.16	0.08	0.08	0.08	0.08	0.11	0.15	0.17
4.12	6.70	5.95	6.04	8.59	4.87	8.28	7.36	6.91	5.26	5.37
0.88	0.68	0.68	0.70	1.13	0.79	0.69	0.63	0.59	0.64	0.74
463652	463497	463664	463793	456234	455839	456010	456100	456500	456289	456750
5400873	5400797	5400597	5400527	5406155	5405704	5405059	5404500	5404050	5403725	5403600
737	750	785	797	5	83	195	292	371	427	449

Table 1 (*continued*).

	OV-13	OV-14	OV-12	OV-10
SiO_2 (wt.%)	52.83	52.19	51.04	51.80
TiO_2	1.46	1.22	1.10	1.18
Al_2O_3	14.16	15.06	15.98	14.91
Fe_2O_3	12.14	11.60	10.83	11.61
MnO	0.26	0.16	0.15	0.15
MgO	5.27	6.00	6.86	6.46
CaO	9.89	10.04	11.25	10.63
K_2O	2.72	2.58	2.19	2.44
Na_2O	1.09	0.97	0.47	0.64
P_2O_5	0.18	0.17	0.13	0.16
Mg#	0.49	0.53	0.58	0.55
Sum	100.20	100.00	99.89	99.87
LOI	0.50	1.40	1.20	1.00
Ti (ppm)	8 736	7 296	6 553	7 085
P	789	752	574	705
Cr	160	148	193	167
Co	50	63	63	59
Ni	35	74	115	77
Rb	23.20	6.82	3.29	8.29
Sr	339	364	360	401
Cs	0.18	0.00		
Ba	436	431	315	450
Sc	41.48	39.55	42.44	43.48
V	335	258	258	301
Ta	1.05	0.95	0.68	0.95
Nb	19.78	18.96	12.91	21.74
Zr	151	127	102	144
Hf	3.83	3.99	2.88	2.90
Th	3.96	3.02	2.00	3.15
U	0.91	0.62	0.40	0.65
Y	27.70	21.42	18.66	24.04
La	24.97	22.80	14.78	20.69
Ce	48.99	44.67	31.37	42.52
Pr	5.90	5.66	3.99	5.43
Nd	22.07	21.03	15.10	19.90
Sm	4.81	4.37	3.54	4.01
Eu	1.55	1.56	1.22	1.32
Gd	5.35	4.77	3.78	4.73
Tb	0.72	0.69	0.54	0.68
Dy	4.77	4.11	3.44	4.09
Ho	0.99	0.86	0.72	0.79
Er	2.97	2.37	1.88	2.13
Tm	0.37	0.34	0.27	0.30
Yb	2.53	2.11	1.70	1.96
Lu	0.38	0.34	0.27	0.26
La/Yb_n	7.08	7.73	6.22	7.56
La/Sm_n	3.36	3.37	2.69	3.34
Gd/Yb_n	1.75	1.87	1.83	1.99
Al_2O_3/TiO_2	9.72	12.36	14.59	12.59
Th/Nb	0.20	0.16	0.15	0.14
Th/La	0.16	0.13	0.14	0.15
Zr/Y	5.45	5.94	5.44	6.00
Nb/Nb	0.58	0.61	0.69	0.81
Easting	457104	456700	457400	457150
Northing	5403188	5403100	5402750	5402400
Height (m)	520	536	596	657

Table 1 (*concluded*).

Note: Major elements were determined for the mafic igneous rocks by X-ray fluorescence spectrometry (XRF), and trace elements, including the REEs and HFSEs, were analyzed using inductively coupled – mass spectrometry (ICP–MS; Perkin Elmer Elan 5000; Table 1) at the Department of Geological Sciences, University of Saskatchewan. Detailed analytical methodology is presented in Fan and Kerrich (1997). Detection limits, defined as 3σ of the procedural blank, for some critical elements, in parts per million, are as follows: Th (0.01), Nb (0.006), Hf (0.008), Zr (0.004), La (0.01), and Ce (0.009). Precision for most elements at the concentrations present in the international reference material BIR-1 is between 2% and 4% relative standard deviations. Chondrite normalized values (e.g., La/Sm_n) are calculated from the values of Sun and McDonough (1989). Anomalies of Nb relative to Th and La are expressed as Nb/Nb* in a manner analogous to Eu/Eu*. Mg# is calculated as $Mg/(Mg + Fe^{2+})$. All samples are from Universal Transverse Mercator (UTM), Zone 16, North American Datum for 1927 (NAD 27). LOI, loss on ignition.

onated HREE. Based on Nd isotopic analysis of crustally derived rhyolites from the North Shore Volcanic Group west of this study area, Vervoort and Green (1997) calculated that the Archean crust underlying the Midcontinent Rift would have formed two isotopic reservoirs at the time of rifting, namely a tonalite–trondhjemite–granodiorite (TTG) member with $\varepsilon_{Nd(1100\ Ma)}$ values of –18 to –13, and a mafic to ultramafic end member with $\varepsilon_{Nd(1100\ Ma)}$ values of –4 to +6. Felsic rocks from the North Shore Volcanic Group have $\varepsilon_{Nd(1100\ Ma)}$ values and incompatible element ratios that are consistent with those of the proposed contaminant (i.e., Archean TTG) in the upper portion of the Osler sequence (Fig. 9). In the vicinity of Rossport (Fig. 1C), Archean granites are exposed along the shoreline, and these are interpreted to underlie the Osler Volcanic Group beneath the islands. Although no geochemical data for these granites are available, the majority of Archean granites exposed in the Superior Province are TTGs with geochemical characteristics similar to those of the proposed contaminant. Although the exact location of the contact between the contaminated and uncontaminated suites is unclear, the ε_{Nd} data combined with Th/La and Th/Nb ratios suggest a marked break at around 400 m, above the base of the section exposed on Vein and Wilson islands (Fig. 5). This supports the models of Shirey et al. (1994) and Nicholson et al. (1997), which suggest that early basaltic magmas (1109–1107 Ma) underwent little interaction with the crust. They suggest that as extension decreases, magma is forced to pond at or near the base of the crust, where it assimilates greater amounts of crustal material. However, the presence of two samples in the upper Osler sequence (OV-30 and OV-35), with higher MgO and compatible trace element contents and trace element ratios that fall within the ranges of lower sequence lavas, indicate that some less contaminated magma was able to rise through, or around, any magma reservoirs within which more contaminated magmas were held.

In a study of the Osler Volcanic Group exposed along the shores of the Black Bay Peninsula (Fig. 1), Lightfoot et al. (1991) proposed that the major and trace element geochemical data could be used to subdivide the flows into upper, central, and lower suites, although the boundaries between these suites are not as clearcut as those between the two suites in this study. Although the geochemical compositions of their central (750–900 m) and upper (900–3000 m) suites overlap,

Table 2. Major and trace element data for the Osler Group sedimentary rocks.

	OS-8	OS-9	OS-4	OS-3	OS-7	OS-5	OS-6	OS-1	OS-2
SiO_2 (wt.%)	53.27	53.38	76.93	75.84	69.74	58.77	57.62	72.66	67.33
TiO_2	1.46	1.36	0.31	0.23	0.81	0.34	0.18	0.24	0.18
Al_2O_3	12.35	12.08	8.91	10.23	10.09	7.11	8.06	11.24	11.09
Fe_2O_3	8.48	7.94	2.93	2.88	6.65	2.16	1.78	3.97	3.82
MnO	0.14	0.13	0.04	0.03	0.05	0.10	0.06	0.04	0.06
MgO	1.97	1.99	0.48	0.40	2.11	2.90	0.62	2.19	2.20
CaO	7.59	7.98	2.52	2.29	1.85	11.14	14.59	1.58	4.86
K_2O	2.31	2.28	3.19	2.81	4.14	4.46	2.00	2.06	2.02
Na_2O	2.54	2.55	0.98	1.97	1.39	0.06	1.75	2.75	2.55
P_2O_5	0.17	0.16	0.11	0.08	0.12	0.10	0.08	0.12	0.11
LOI	9.65	10.08	3.57	3.19	2.97	12.79	13.22	3.12	5.75
Sum	99.94	99.94	99.95	99.95	99.92	99.93	99.96	99.95	99.96
Cr (ppm)	43.71	38.96	27.58	29.85	127.57	22.77	32.56	39.64	42.51
Ni	44.22	39.67	16.96	15.22	45.99	12.98	16.31	28.50	28.60
Rb	82.11	79.50	86.14	73.49	121.87	98.31	62.23	67.79	68.58
Sr	675.3	743.2	56.1	82.0	82.8	75.9	131.5	109.3	105.2
Cs	3.026	2.807	1.860	1.465	2.826	2.999	1.526	1.204	1.183
Sc	20.41	19.01	5.22	5.73	12.38	7.06	3.73	4.55	4.63
V	152.44	144.33	22.80	23.47	63.30	30.06	25.79	50.19	42.95
Ta	0.67	0.66	0.53	0.29	0.86	0.55	0.30	0.32	0.31
Nb	12.4	12.6	7.6	3.8	13.5	8.1	3.7	5.5	3.8
Zr	205.9	198.6	206.7	94.9	220.4	287.3	100.6	151.7	85.2
Hf	5.3	5.1	5.1	2.4	6.0	7.4	2.6	3.9	2.2
Th	4.94	5.04	5.50	2.69	8.06	10.07	3.10	3.57	2.40
U	1.032	0.993	1.120	0.756	2.070	2.196	0.972	1.131	0.868
Y	24.61	23.71	17.43	11.42	28.89	23.75	12.70	17.09	16.26
La	41.92	39.96	17.04	12.94	33.14	23.79	12.48	14.53	15.86
Ce	65.23	62.50	29.22	24.39	70.08	56.25	20.05	23.78	25.60
Pr	9.472	9.049	4.075	3.347	8.072	6.925	2.967	3.595	3.836
Nd	35.77	34.14	15.92	13.48	31.52	28.18	11.85	14.37	15.79
Sm	6.61	6.32	3.62	2.78	6.40	5.67	2.42	3.04	3.28
Eu	1.581	1.497	0.820	0.665	1.343	0.996	0.572	0.744	0.822
Gd	5.529	5.314	3.407	2.472	5.642	4.823	2.299	2.998	3.248
Tb	0.822	0.788	0.526	0.362	0.883	0.717	0.345	0.468	0.491
Dy	4.815	4.712	3.151	2.082	5.500	4.282	2.083	2.897	2.872
Ho	0.949	0.908	0.626	0.419	1.098	0.850	0.417	0.587	0.574
Er	2.676	2.603	1.839	1.195	3.216	2.519	1.230	1.670	1.610
Tm	0.374	0.360	0.268	0.169	0.465	0.363	0.172	0.231	0.229
Yb	2.44	2.39	1.84	1.13	3.13	2.48	1.12	1.50	1.54
Lu	0.358	0.346	0.275	0.167	0.460	0.372	0.170	0.230	0.231
Easting	423500	423500	446000	446000	456700	461800	461900	472100	472000
Northing	5489800	5489800	5409500	5409500	5403800	5404200	5404000	5402000	5402100

Note: All samples are from UTM, Zone 16, NAD 27.

their lower suite (0–750 m) is distinguished by elevated Mg numbers (0.55–0.70 versus 0.30–0.60), lower Al_2O_3 (8–12 wt.% versus 13–17 wt.%), lower Th/Nb ratios (0.09–0.70 versus 0.30–0.60), but higher Gd/Yb_n ratios (3.5–4.5 versus 1.6–2.6). When compared with the data from this study, it can be seen that samples from below 400 m are comparable to those from the lower suite, and samples above the interval are similar to those from the central suite (Fig. 8C). This suggests that the flood basalts of the Osler Group thin to the east as a result of either local or regional variations in the topography. This agrees with the unconformity at the base of the Osler Group requiring that the underlying block rotated down to the west and was erosively beveled in the east prior to deposition of the basal Osler, as well as paleocurrents in

Fig. 4. Plots of MgO, Fe_2O_3, TiO_2, and Th versus SiO_2 for igneous rocks from Vein and Wilson islands.

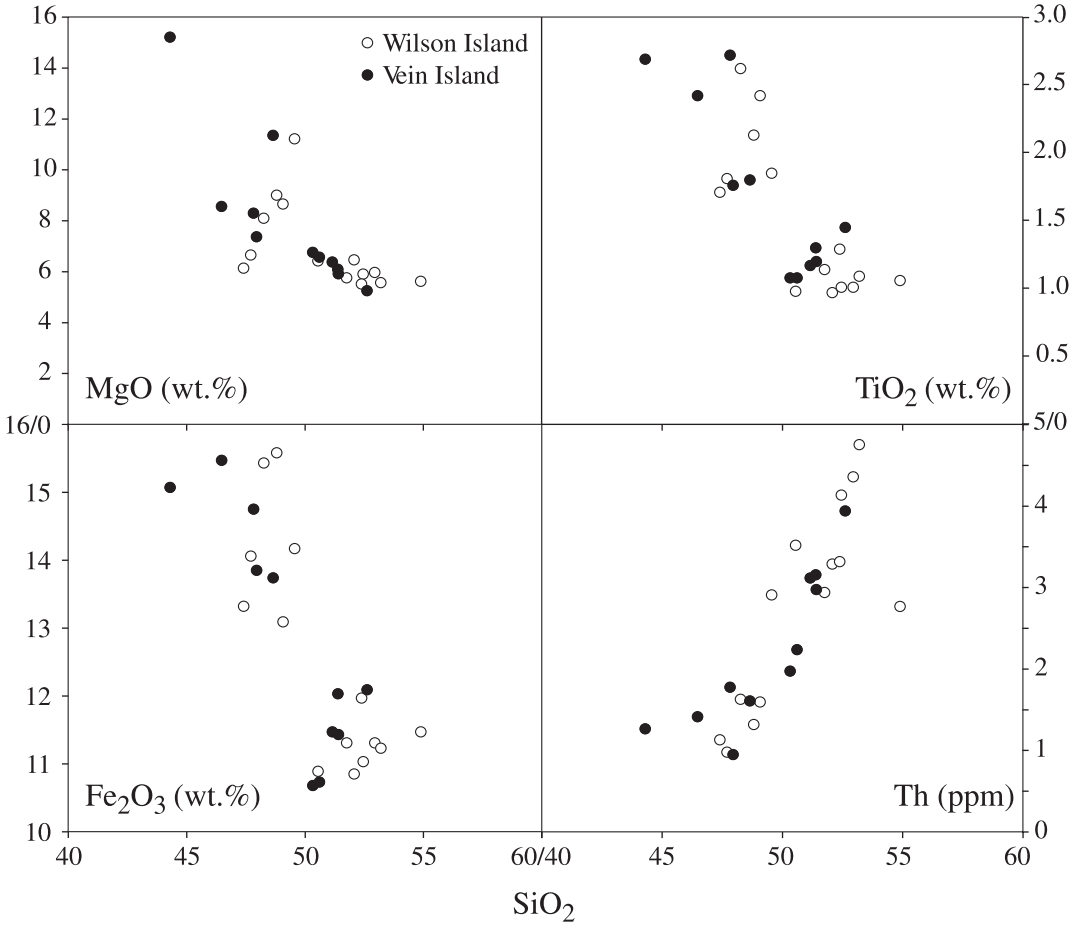

Fig. 5. Geochemical stratigraphy of the Osler Group on Vein (solid circles) and Wilson (open circles) islands. The stratigraphic position of the samples has been calculated assuming a dip of 10° parallel to the section. Zero is taken as the top of the Simpson Island Formation. Sample locations are shown in Fig. 1.

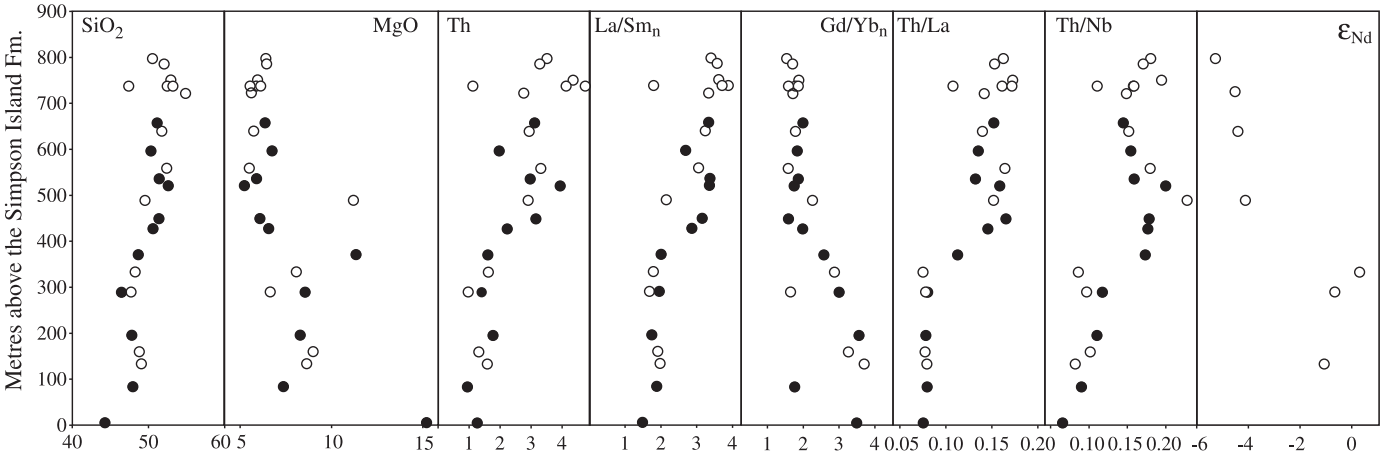

the Simpson Island Formation, which indicate that the regional paleoslope was down to the west when the lower Osler was being erupted.

Lightfoot et al. (1991) concluded that neither varying degrees of partial melting nor fractionation of plagioclase, olivine, and pyroxene could account for the observed trends in their data set. Rather, they invoked crustal contamination to account for the observed trends, proposing a model of simple mixing followed by only a minor amount of fractionation after contamination. Lightfoot et al. (1991) interpreted the data from their central suite, where the most contaminated magmas appear at the base of the suite, to indicate that they formed from a crustal-level magma chamber, which was geochemically stratified by fractionation and contami-

Table 3. Radiogenic isotope data for Osler Group volcanic rock.

	OV-2	OV-2 (duplicate)	OV-6	OV-7	OV-35	OV-31	OV-32	OV-25
Measured $^{143}Nd/^{144}Nd$	0.512165	0.512165	0.512286	0.512260	0.512045	0.511905	0.511913	0.511857
Uncertainty (2σ)	0.000012	0.000014	0.000010	0.000012	0.000010	0.000008	0.000010	0.000010
$^{147}Sm/^{144}Nd$	0.1391	0.1390	0.1528	0.1424	0.1440	0.1276	0.1278	0.1262
Initial $^{143}Nd/^{144}Nd$	0.511156	0.511156	0.511177	0.511226	0.511000	0.510979	0.510985	0.510941
$\varepsilon_{Nd(1100\ Ma)}$	–1.06	–1.05	–0.65	0.31	–4.11	–4.51	–4.40	–5.27
T_{dm} (Ma)	1926	1924	2057	1815	2320	2125	2118	2175
Present-day $^{87}Sr/^{86}Sr$	0.704039		0.704763	0.704482	0.707526	0.709219	0.706384	0.708981
Uncertainty (2σ)	0.000016		0.000016	0.000014	0.000014	0.000017	0.000019	0.000012
$^{87}Rb/^{86}Sr$	0.022699		0.033332	0.078412	0.138012	0.068172	0.063993	0.032739
Initial $^{87}Sr/^{86}Sr$	0.703680		0.704235	0.703241	0.705341	0.708140	0.705371	0.708463
Height (m)	133	133	290	333	489	639	639	797

Note: Radiogenic isotope analyses were performed at Carleton University, Ottawa. Total procedural blanks for Sr were < 450 pg. Isotope ratios were normalized to $^{86}Sr/^{88}Sr = 0.11940$ to correct for fractionation. Two standards were run at Carleton, namely NIST SRM987 ($^{87}Sr/^{86}Sr = 0.710251 \pm 18$, $n > 50$, September 1992 – August 2004) and the Eimer and Amend (E&A) $SrCO_3$ ($^{87}Sr/^{86}Sr = 0.708032 \pm 24$, $n > 20$, September 1994 – August 2004). Total procedural blanks for Nd were < 350 pg. Concentrations are precise to ±1%, and $^{147}Sm/^{144}Nd$ ratios are reproducible to 0.5%. Isotope ratios were normalized to $^{146}Nd/^{144}Nd = 0.72190$. Analyses of the US Geological Survey standard BCR-1 yield Nd = 29.02 ppm, Sm = 6.68 ppm, and $^{143}Nd/^{144}Nd = 0.512668 \pm 20$ ($n = 4$). Fifty-four runs were taken of the La Jolla standard average $^{143}Nd/^{144}Nd = 0.511876 \pm 18$ (September 1992 – February 2004). T_{dm}, depleted-mantle model age.

nation and then tapped from the top downwards. The lower suite is interpreted to have been formed from a distinct and more primitive source than that of the central and upper suites, consistent with an enriched asthenospheric upper mantle source, whereas the central and upper suites were interpreted to be melts of a more depleted source that have interacted with continental upper crust. This is consistent with our data from Vein and Wilson islands. The depleted upper mantle (i.e., the source of mid-ocean-ridge basalts) cannot be the source for lower suite lavas of the Osler Group, however, since they have ε_{Nd} values less than that of depleted mantle but show little evidence for contamination.

Nicholson et al. (1997) concluded that there were five geochemically distinct flood-basalt compositions within the Midcontinent Rift that are common to most sections and appear in approximately the same stratigraphic order (shown by Roman numerals in Fig. 10). Nicholson et al. recognized a lower suite in the Siemens Creek Volcanics (basalt type 1; Fig. 10), which they suggest is analogous to the lower suite of Lightfoot et al. (1991). In Minnesota this unit is < 100 m thick, whereas the lower suite of the Osler Group of Lightfoot et al. (1991) is ~750 m thick. They report a narrow range of $\varepsilon_{Nd(1100\ Ma)}$ values for the Siemens Creek Volcanics of –0.7 to +0.7. Nicholson et al. further suggest that there is a broadly recognizable suite of basalts above this (basalt type II), which includes the upper Siemens Creek Volcanics (Fig. 10). The suite is characterized by slight negative Nb anomalies and a range of $\varepsilon_{Nd(1100\ Ma)}$ values of –1.4 to –6.9. They suggest that type II may be analogous to the most primitive members of the central suite of Lightfoot et al. (1991). Our data from the Lower Osler sequence are comparable with those of Nicholson et al. for the lower Siemens Creek Volcanics of upper Michigan and northwest Wisconsin (Fig. 10).

The well-developed exposure of Midcontinent Rift flood basalts at Mamainse Point comprises a ~5250 m thick sequence of over 350 individual flows ranging in composition from picrite to basaltic andesite and is thought by many authors to represent the most complete section of Keweenawan-age basalts preserved on the shores of Lake Superior. As such, this has been the subject of detailed studies (Klewin and Berg 1990, 1991; Shirey et al. 1994; Shirey 1997). The age of the sequence is unclear but has been interpreted by Shirey et al. (1994) to range from 1108 to 1088 Ma. Klewin and Berg (1991) proposed that geochemical variations in the eight suites they recognized were consistent with lavas becoming less primitive as the depth of melting of the mantle source decreased. The majority of their samples, however, particularly those from the basal suite, are characterized by distinct negative Nb and Ta anomalies, unlike basalt samples from this study. The Mamainse Point basalts display a range of $\varepsilon_{Nd(1100\ Ma)}$ values of +3.4 to –9 (Shirey et al. 1994). The lowermost flow units have $\varepsilon_{Nd(1100\ Ma)}$ values of –1 to –5, with the highest value (–1) at the top of the sequence. Farther up section, values become increasingly more negative, reaching –9 at a height of ~2400 m. Re–Os-isotope data from the Mamainse Point picrites suggest that primary magmas interacted with older subcontinental lithospheric mantle with low ε_{Nd} (Shirey 1997). The lowermost basalts of the Osler Group are isotopically distinct from the lowermost

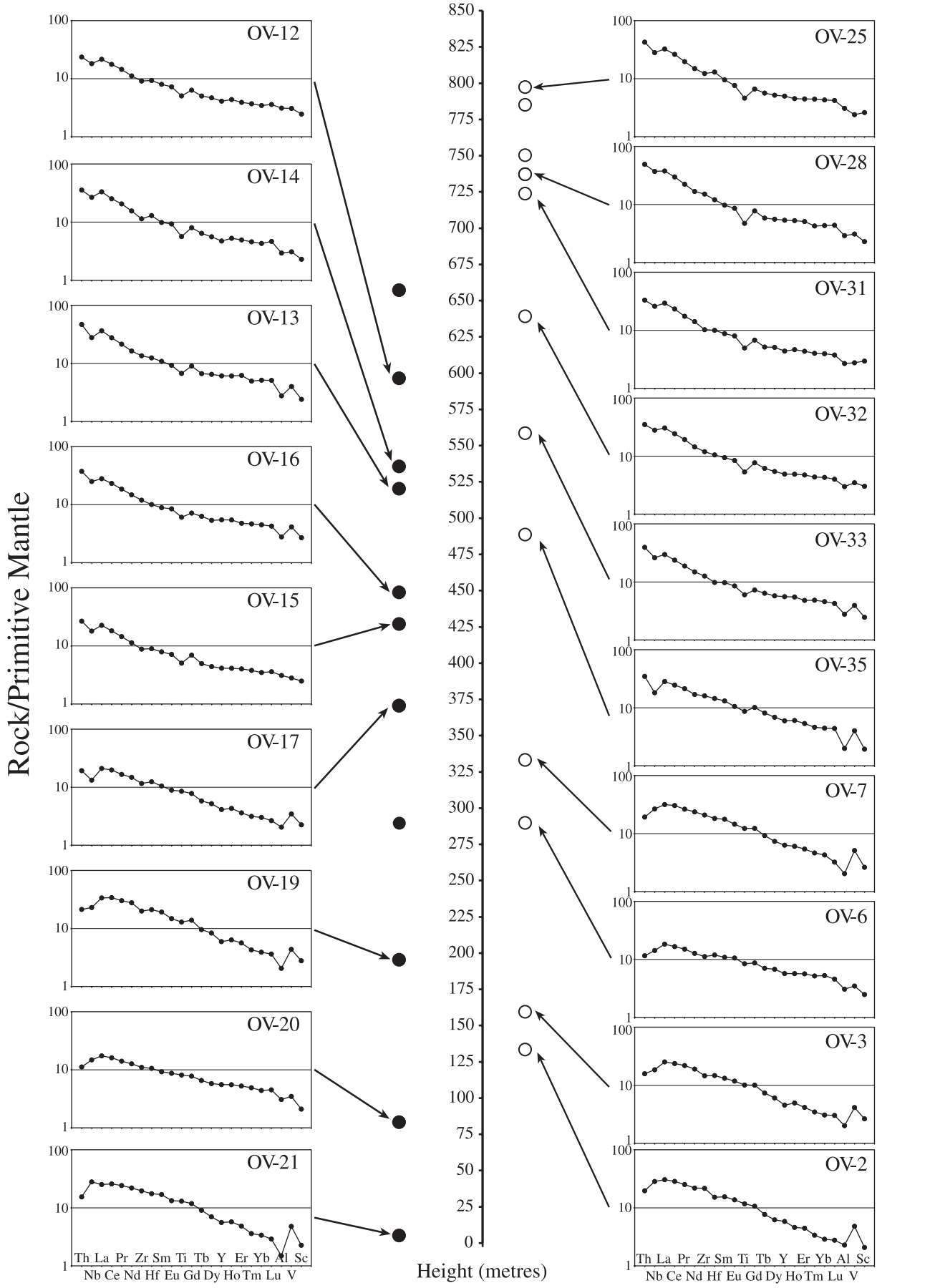

Fig. 6. Representative primitive mantle normalized diagrams of samples of the Osler Group basalts showing variations with height above contact with the top of the Simpson Island Formation. Normalizing values are those of Sun and McDonough (1989).

Fig. 7. (A, B) Sandstone geochemistry of layers in various sedimentary units of the Osler Group. The stratigraphic sections are not to scale. Division by Al_2O_3 is used to normalize and correct for varying amounts of quartz in the samples (Fralick 2003). First-row transition element enrichment in the stratigraphically highest three samples is depicted in (A), and the upper sample from the lower member and, especially, the lower sample from the upper member are shown in (B) as being enriched in HFSE.

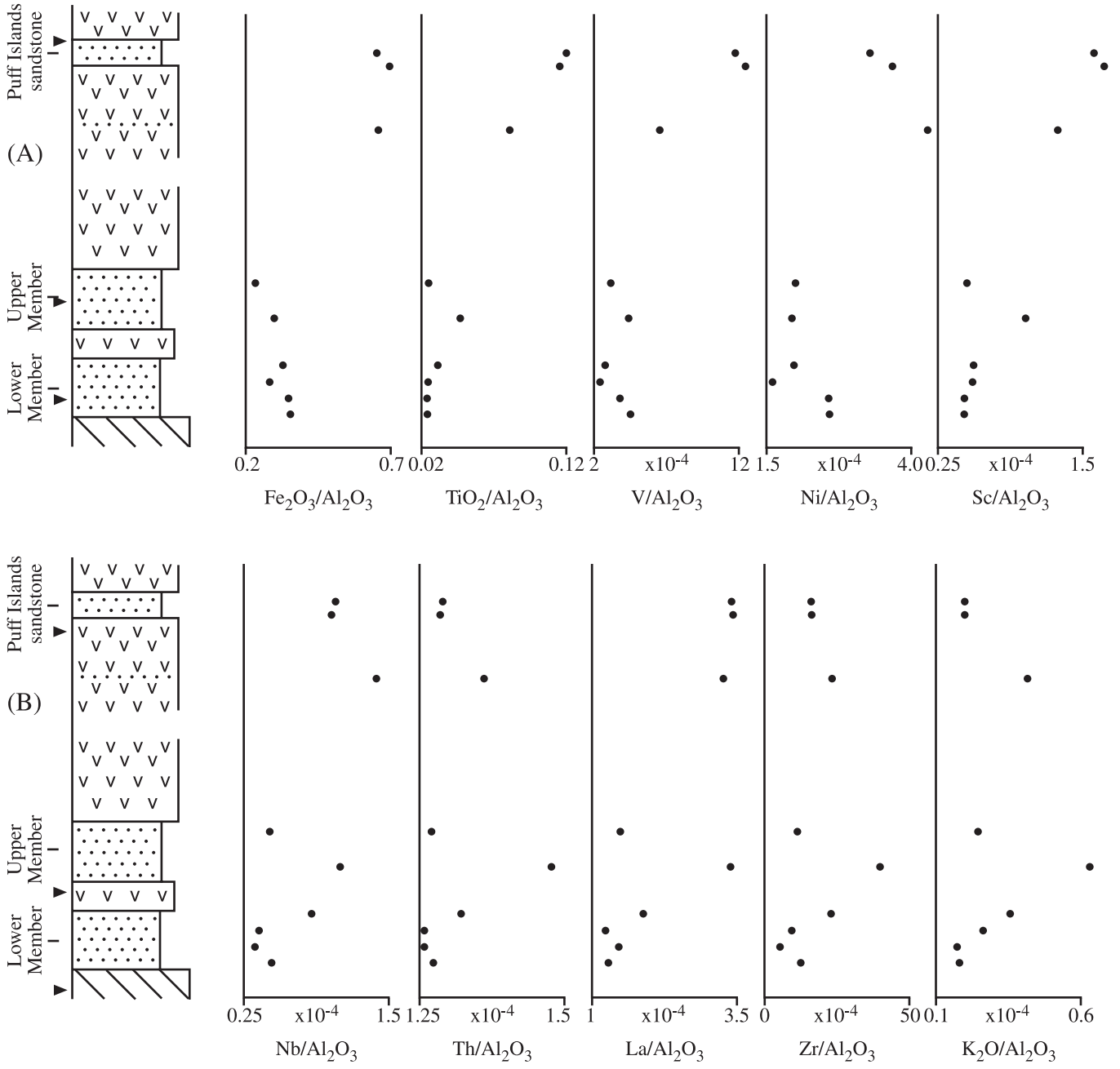

units of Mamainse Point, indicating that geochemical correlation of the lowermost volcanic packages around the rift margins may not be possible.

Geochemical results for the sedimentary units corroborate the provenance of the detritus as determined by examination of clast lithologies. The geochemical data add more detail to the conclusions, however. The majority of samples from the Simpson Island Formation are similar in composition to the underlying Sibley Group sandstones (Fig. 11). Much less Archean detritus is present in these sandstones than appears as clasts in the conglomerates. This may be because the Archean lithologies are more resistant to physical abrasion, leading to their concentrating in the larger grain sizes. Two of the samples from the Sampson Island Formation have

Fig. 8. Comparison of primitive mantle normalized plots from the Osler Group with (A) Phanerozoic ocean-island basalt (OIB) and continental flood basalts (CFB) and with (B, C) the lower and central suites of Lightfoot et al. (1991). Types 1 and 2 basalts are from the lower and upper Siemens Creek Volcanics of Nicholson et al. (1997). CFB data are from Gibson et al. (2000), and OIB data from Frey et al. (1990).

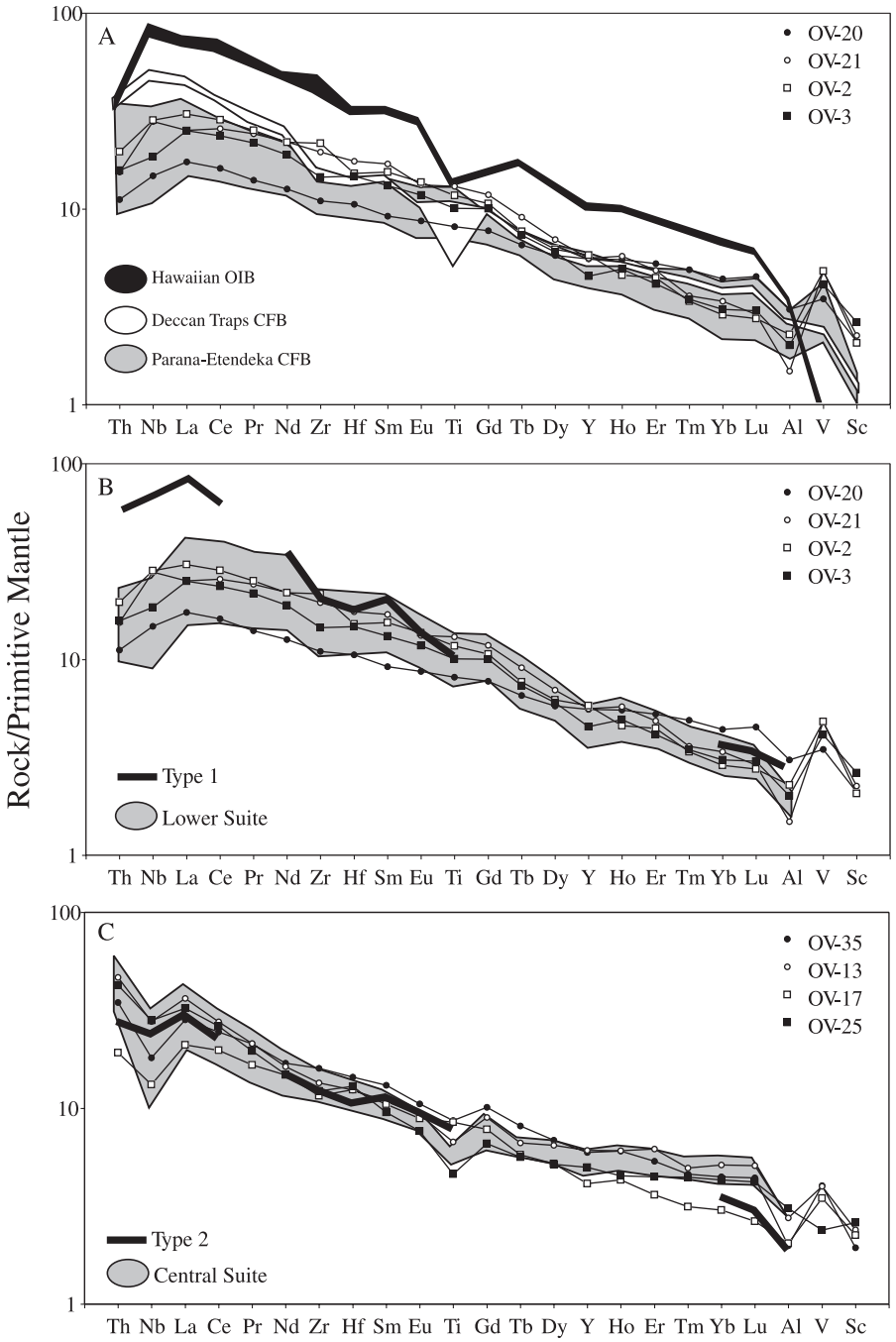

considerable amounts of detritus with a composition consistent with derivation from rift-related felsic volcanic rocks mixed with the Sibley Group derived detritus (Fig. 11). This is reasonable because the upper member sample is slightly above the 1108 Ma quartz porphyry and the lower member sample is probably at the same stratigraphic level as the porphyry. The three sandstone samples from the upper half of the Osler Group have a very different geochemistry than that of the stratigraphically lower samples. They can be modeled as a mixture of detritus derived from felsic and mafic rift-related volcanic rocks (e.g., the thin interflow sandstone sample) or composed completely of mafic rift volcanic detritus (e.g., the Puff Island samples). These data further highlight that sediment deposited in the upper Osler Group had an intrabasinal source.

Depositional system

The Simpson Island Formation is composed of a laterally continuous sedimentary succession up to 25 m thick and dis-

Fig. 9. Plot of La/Sm versus $\varepsilon_{Nd(1100\ Ma)}$, highlighting similarities between rocks from the Osler Group and those from other volcanic and intrusive sequences from the margins of the Midcontinent Rift. Data are from Paces and Bell (1989), Nicholson and Shirey (1990), Shirey et al. (1994), Thériault et al. (1997), Vervoort and Green (1997), and Wirth et al. (1997). Pen., Peninsula; Pt., Point; Volc., volcanic.

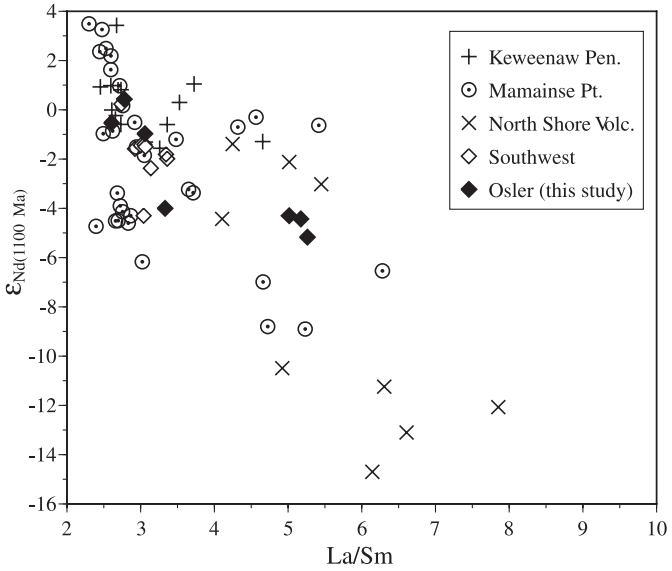

continuous sedimentary units up to 30 m thick interlayered with the basal basalt flows. The lowest sedimentary beds fill channelways cut into underlying sandstones of the Sibley Group. Channel fills and the overlying sedimentary assemblage represent a braided stream system, similar to the South Saskatchewan model (Miall 1978). In this model, dunes composed of coarse-grained sand migrated down the channels and gravelly, longitudinal bars with chute channels and bar-edge sand wedges form the higher relief areas (Fig. 3). The fluvial interpretation is consistent with Tanton (1931) and McIlwaine and Wallace (1976).

Clast lithologies and geochemistry indicate debris was derived mainly from erosion of local basement rocks. A possible exception is red granite clasts in the Copper Island portion of the sedimentary assemblage that yielded U–Pb zircon ages of approximately 1600 Ma (Davis and Sutcliffe 1985), indicating that pre-rift, igneous, Mesoproterozoic rocks may be present in the area, though none crop out at present. Intrusive rocks dated at ~1590 Ma have recently been recognized to the northwest of Lake Nipigon (Heaman and Easton 2005). After deposition of the lower member and eruption of a few tens of metres of basalt, erosion of the Sibley Group resulted in quartz arenite debris from this source dominating the assemblage (Fig. 3, section 5). Such a drastic change in clast composition infers tectonic adjustment of the terrain rather than progressive erosive downstripping as the causative factor. This change in the source area is not reflected by the clast lithologies of the interflow sedimentary assemblage of section 6 (Fig. 2), from which it could be concluded that section 6 is slightly older than section 5. The coarsening-upwards deltaic deposits of section 6 imply that the underlying thin sequence of basalt flows dammed the fluvial system, creating a depression into which the delta was deposited.

Paleocurrent indicators in all these units show flow to the west, with the higher variance in section 6 being caused by the distributary nature of the small delta and wave reworking of sediments. Hamblin (1965) and Franklin (1970) also reported paleocurrents directed towards the west. Total erosive removal of the underlying upper two formations of the Sibley Group in the eastern outcrop areas, while ~400 m of this succession underlies the Osler Group in the west, also implies a protracted period of westward tilt prior to deposition of the Simpson Island Formation of the basal Osler Group.

Sedimentary rocks on Puff Island are probably substantially younger (more than 2 Ma) than the Simpson Island Formation and are totally sourced within the rift. The presence of caliche denotes a semiarid climate, and the interlayering of incised braided fluvial, mass-flow, and sheetflood deposits (Fig. 3) implies the setting was probably the upper mid-fan area of an alluvial fan. Transverse drainage into the rift, indicated by paleocurrent measurements, agrees with the alluvial fan interpretation. Halls (1974) notes that in other areas where the magnetic reversal has been identified, a coarse-grained sedimentary assemblage commonly separates the volcanic units. Thus, this sedimentary package may represent a basin-wide hiatal surface (Halls 1974).

Tectonic model

Accumulation of the Osler Group began with the development of a trunk stream flowing to the west, parallel with the present-day rift axis (Fig. 12). This represents either longitudinal drainage in the rift with stream confinement caused by an upraised block to the south or a regional westward-dipping paleoslope developed prior to extensive subsidence to the south along the major rift axis. The westward thickening of the lower volcanic unit, the erosive removal of ~400 m of the underlying Sibley Group in the eastern portion of the study area, and the westward-dipping Archean–Proterozoic unconformity clearly visible on a seismic line (fig. 7 of Cannon et al. 1989) shot ~90 km to the south-southeast of the study area support the latter. The area to the west, towards which the paleosurface was tilted, makes up the southern portion of the Nipigon Embayment. This is a Mesoproterozoic linear trough extending northward from ~18 km west of the study area and bounded on its eastern margin by the Black Sturgeon Fault. The trough is filled with ~400 m of continental sedimentary rocks (lower Sibley Group, between 1620 and 1340 Ma) and 500 m of ~1109 Ma sills. The intrusions in this area represent the first igneous pulse related to the rift. The older mafic–ultramafic intrusions (e.g., the Seagull intrusion) are geochemically comparable to modern OIB and are characterized by ε_{Nd} values that are generally positive (Heggie 2005). In contrast, the slightly younger diabase sills in this area are comparable to OIB-related rocks but display geochemical (e.g., negative Nb anomalies) and isotopic (negative ε_{Nd} values) characteristics of crustal contamination (Richardson and Hollings 2005). Faults that offset the intrusions indicate that the graben was active after emplacement of Midcontinent Rift sills (Hart et al. 2005). Any extensions of these faults to the south do not

Fig. 10. Schematic correlations of volcanic rocks of the Midcontinent Rift based on the stratigraphic position of distinctive basalt sequences, magnetic polarity, and absolute age where possible. Modified after Nicholson et al. (1997). Broken lines in the upper Michigan section separate lower and upper members of Kallander Creek and Siemens Creek volcanics. The left-hand column shows magnetic polarity (N, normal; R, reversed). Roman numerals I–IV refer to five distinctive, laterally extensive basalt compositions identified on the south shore of western Lake Superior. Where equivalent basalt compositions occur in other stratigraphic successions, the appropriate Roman numeral is noted (see Nicholson et al. 1997 for data sources). Shaded regions represent intervals in which contacts are covered or obscured by plutonic rocks.

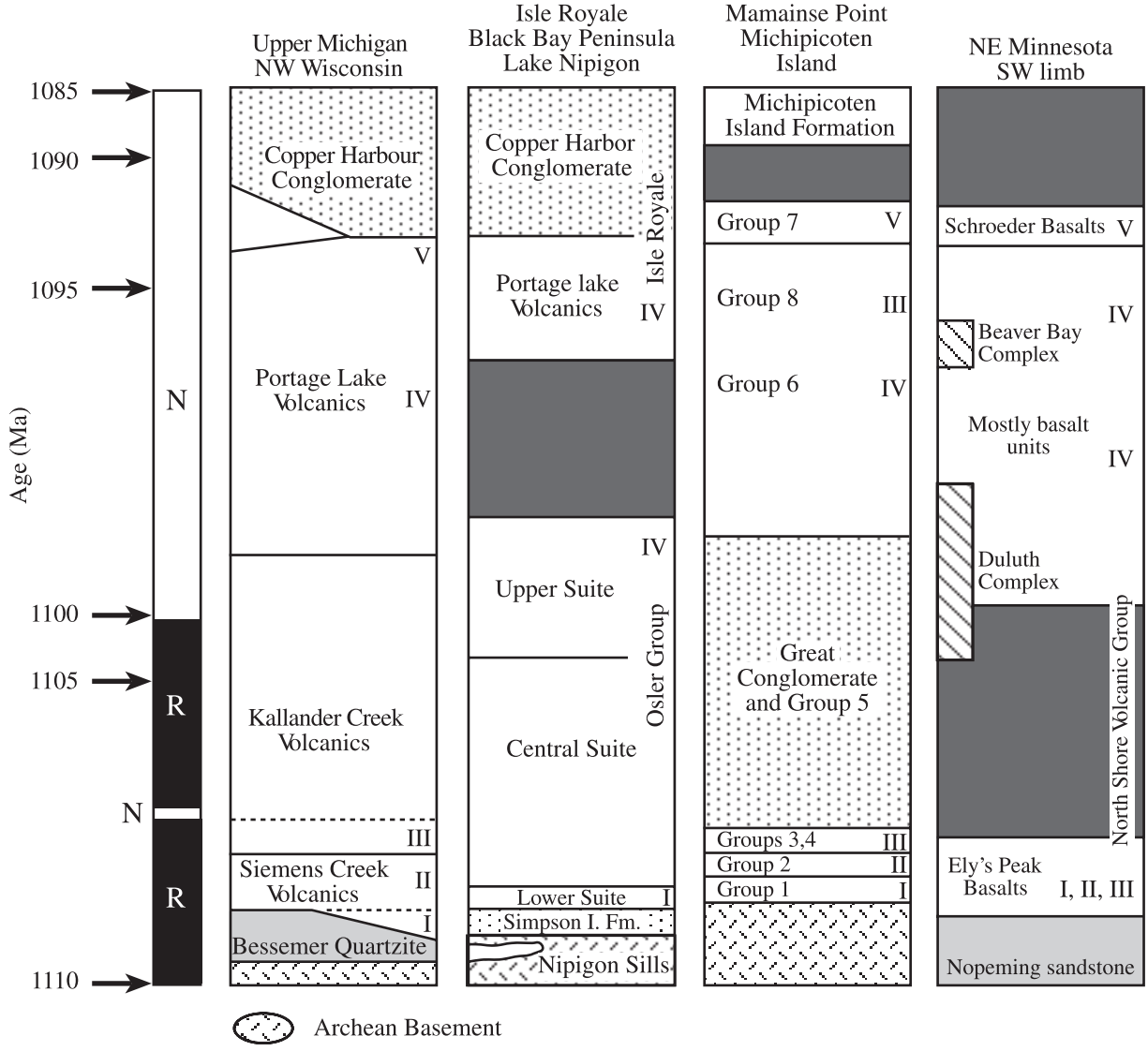

propagate through the Osler Group, however. This implies that the Nipigon Embayment was subsiding during sill emplacement, and the slightly younger sediments and lavas of the Osler Group flowed towards this down-thrown area (Fig. 12). This is consistent with the uncontaminated nature of the mafic–ultramafic intrusions, which suggest higher extension rates. The preweakened crust underlying the Nipigon Embayment and its alignment with the western arm of the Midcontinent Rift probably promoted the initiation of magmatism and subsidence in this area.

Thin, sandstone-dominated assemblages underlie other ~1108 Ma basal volcanic units on the west arm of the Midcontinent Rift. The reversely magnetized Ely's Peak basalts on the southwest limb of the North Shore Volcanic Group are underlain and intercalated with fluvial clastic rocks of the Nopeming Formation (Fig. 10). Strata of the northeast limb of the North Shore Volcanic Group are underlain by the Puckwunge Formation, and the Powder Mill Group is underlain by the Bessemer quartzite. Quartz arenites are common to all these sedimentary packages (Ojakangas and Morey 1982*a*), possibly denoting recycling from erosion of sandstones similar to the Sibley Group quartz arenites. Paleocurrent trends are diverse, with only the Puckwunge Formation showing transverse flow towards the rift axis (Ojakangas and Morey 1982*a*). Again, it appears that the major rift trend was not the feature controlling subsidence during this earliest phase of basin development. Localized paleoslopes, possibly aligned by zones of pre-existing

crustal weakness, appear to be the dominant regime. The lack of far-traveled detritus implies that the region surrounding the localized areas of subsidence may have been domed due to higher than average heat flow. The lower succession of less contaminated basalts was erupted in this setting (Fig. 12). These basalts are interpreted to have been derived from a mantle plume source and to have ascended to the surface with little or no interaction with the country rocks. This is consistent with higher rates of extension which allow magma to ascend rapidly through the lithosphere.

By the time the Puff Island alluvial fan sediments were being deposited, the paleoslope had rotated to a southeasterly dip towards the axis of the Midcontinent Rift (Fig. 12). This is consistent with interflow sedimentary assemblages throughout the Lake Superior region of the rift, which almost invariably contain indicators showing flow that is transverse to the rift axis (Merk and Jirsa 1982). Similarly, many of these successions are derived exclusively from intrabasinal or intrarift igneous rocks (Merk and Jirsa 1982), indicating cannibalization of internal highlands, suggesting extensive block faulting, restricted access of major drainage systems, and probable existence of a thermal welt. The period between 1108 and 1105 Ma marks a changeover in the organization of the northern segment of the rift from a more regional paleoslope tilted towards the Nipigon area to development of the block-faulted rift trough. The upper sequence of the Osler Group volcanic basalts is characterized by negative Nb anomalies and ε_{Nd} values that are best interpreted as the result of contamination by Archean basement rocks. This can be interpreted as the result of a decrease in the rate of rifting, which resulted in increased crustal residence times for the upwelling magmas. The switch from uncontaminated basalts at the base of the sequence to contaminated ones near the top occurs at around 400 m above the lower sedimentary sequence. It is difficult to determine if the block rotations necessary to accomplish the change in the paleoslope occurred only slightly prior to the deposition of the Puff Island alluvial fan or are represented by a lower stratigraphic interval marked by the change from uncontaminated to contaminated volcanism. However, the change in the paleoslope implies a reorientation of the tectonic forces, which could account for the increased crustal residence time of the contaminated magmas. The lack of correlation between the Osler Group volcanic rocks and the other sequences around the rift suggests that this may have been a localized event.

Conclusion

The sedimentology and geochemistry of the Osler Group provide significant insights into the early phases of the Midcontinent Rift. The sedimentary rocks of the Simpson Island Formation indicate that the early phases of rifting (pre-1108 Ma) took place along a north–south axis, possibly along long-lived crustal-scale faults recognized in the Nipigon Embayment. Later phases of rifting involved subsidence along an east–west axis. The transition between the two phases is coincident with a change in the geochemical signature of the Osler basalts and an increase in the crustal contamination signature of the magmas. This is consistent with the early, mafic to ultramafic flows being transported through the lithosphere with relatively little interaction with continental crust, possibly utilizing the large-scale crustal faults as conduits, whereas later magmas underwent longer residence times within the crust, possibly as a result of the shifting stress field required to reorientate the rift axis.

Fig. 11. Ratio plot comparing Osler Group sandstone geochemistry with that of the four major possible source rocks. More HFSE-enriched compositions plot higher in the diagram, and more mafic compositions plot farther to the right in the diagram. The Quetico metasandstone samples are representative of the Archean rocks in the area, as these were their source (Fralick and Kronberg 1997). The data for the Osler Group mafic volcanic rocks are from this paper. The typical felsic Midcontinent Rift igneous rock is from Sutcliffe (1991). The Quetico and Sibley data are unpublished. Error bars on the average compositions represent one standard deviation.

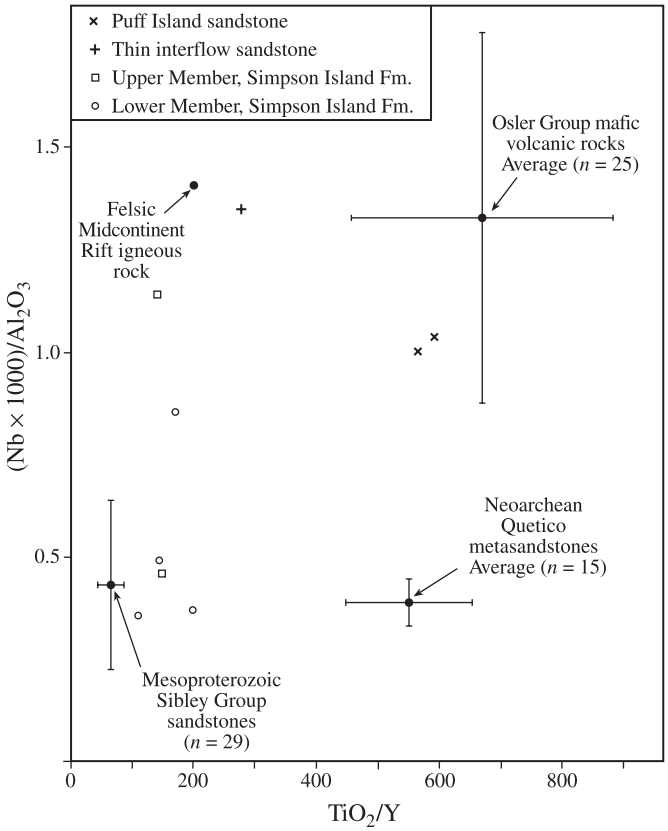

Acknowledgments

The authors are grateful for technical assistance from Anne Hammond and Sam Spivak. This research was funded in part by Natural Sciences and Engineering Research Council of Canada Discovery Grants to PH and PF. Early drafts of this manuscript benefited from comments by M. Jirsa and M. Easton. Constructive reviews by J. Chiarenzelli and P. Corcoran and Associate Editor W.J. Davis improved the manuscript.

Fig. 12. Schematic diagrams depicting evolution of the northern Midcontinent Rift during its early history. (A) At ~1113–1109 Ma, large volumes of diabasic magma intruded Proterozoic sedimentary rocks and Archean basement in the vicinity of Lake Nipigon. These, and associated mafic–ultramafic intrusions, are the oldest known igneous rocks associated with the rift. The area of intrusive activity was undergoing subsidence at this time as denoted by river systems flowing towards this region (detail a), even though the upper crust was inflated in places in excess of 0.5 km by the sill complex (Rogala et al. 2005). The prefractured nature of the basement in this area, which contains normal faults developed during a previous interval of Mesoproterozoic extension related to the deposition of the Sibley Group (Rogala et al. 2005), may have served to promote early rift igneous activity in the Lake Nipigon region. The beginning of rift-related volcanism in this region (detail a′) is represented by relatively uncontaminated magmas of the early Osler Group. Sedimentary units intercalated with these flows indicate subsidence was continuing to the west in the Nipigon area. The formation of the rift proper did not commence until ~1106–1005 Ma (B) with rotation of basement blocks to the southeast. At approximately this time interval, magmas became more contaminated by continental crust, indicating more interaction with continental crust and possibly longer crustal residence times. The eruption of felsic melts and a hiatus accompanied by the development of alluvial fans (detail b) attest to the heating of the crust during the final phase of this initial period of volcanism followed by a hiatus in igneous activity. The lack of extrabasinal detritus in the alluvial fans implies the formation of a thermal dome isolating the basin from the continental drainage system.

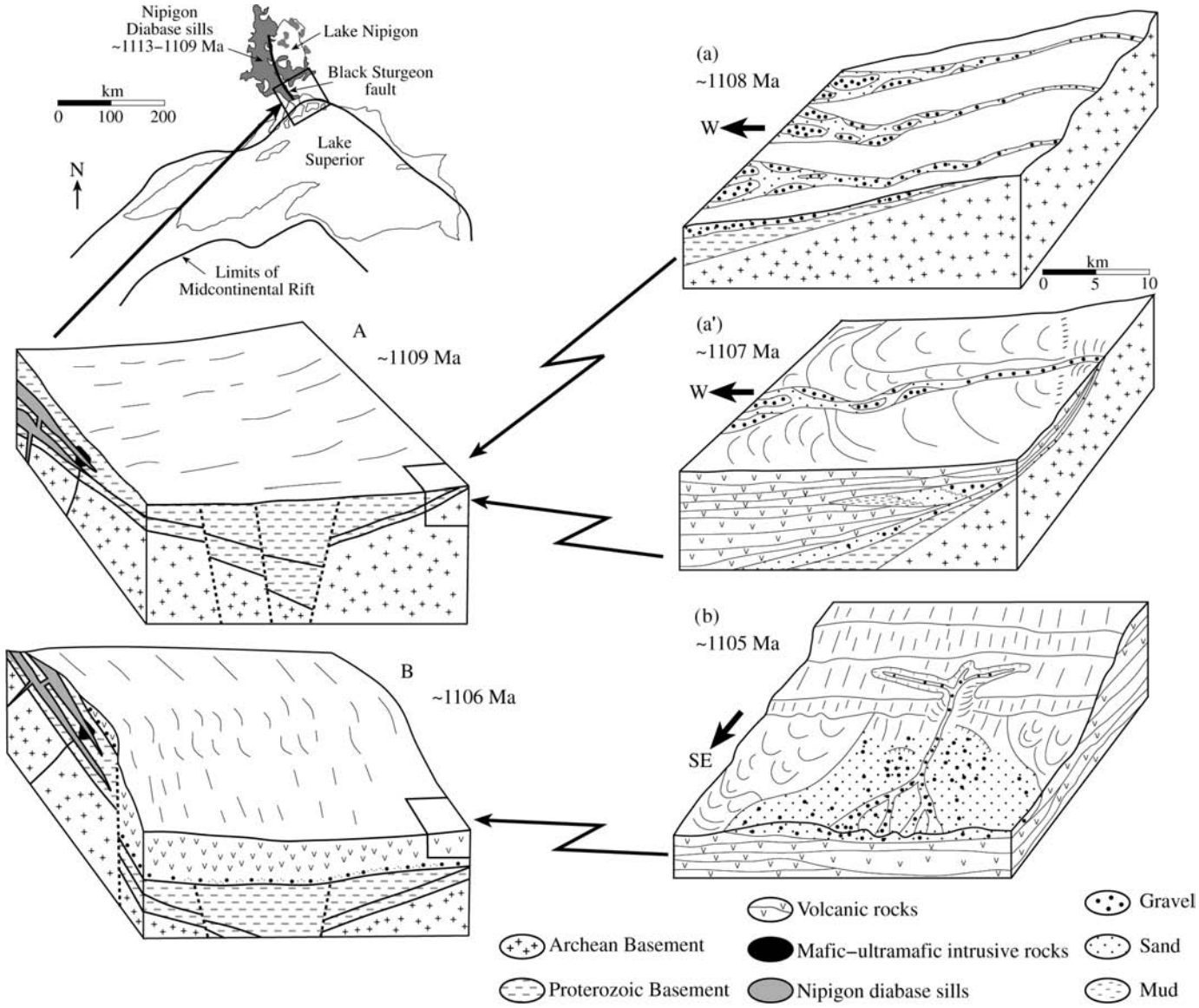

References

Behrendt, J.C., Hutchinson, D.R., Lee, M., Thornber, C.R., Tréhu, A., Cannon, W., and Green, A. 1990. GLIMPCE seismic reflection evidence of deep-crustal and upper-mantle intrusions and magmatic underplating associated with the Midcontinent Rift system of North America. Tectonophysics, **172**: 595–615.

Boothroyd, J.C., and Ashley, G.M. 1975. Processes, bar morphology, and sedimentary structures on braided outwash fans, northeastern Gulf of Alaska. *In* Glaciofluvial and glaciolacustrine sedimentation. *Edited by* A.V. Jopling and B.C. McDonald. Society of Economic Paleontologists and Mineralogists, Special Publication 23, pp. 193–122.

Cannon, W.F. 1992. The Midcontinental rift in the Lake Superior region with emphasis on its geodynamic evolution. Tectonophysics, **213**: 41–48.

Cannon, W.F. 1994. Closing the Midcontinental rift — a far-field effect of Grenvillian compression. Geology, **22**: 155–158.

Cannon, W.F., and Hinze, W. 1992. Speculations on the origin of the North American Midcontinent rift. Tectonophysics, **213**: 49–55.

Cannon, W., Green, A., Hutchinson, D., Lee, M., Milkereit, B., Behrendt, J., Halls, H., Green, J., Dickas, A., Morey, G., Sutcliffe, R., and Spencer, C. 1989. The North American Midcontinent Rift beneath Lake Superior from GLIMPCE seismic reflection profiling. Tectonics, **8**: 305–332.

Catacosinos, P.A. 1981. Origin and stratigraphic assessment of Pre-Mt. Simon clastics (Precambrian) of Michigan Basin. American Association of Petroleum Geologists Bulletin, 65(9): 1617–1620.

Chase, C.G., and Gilmer, T.H. 1973. Precambrian plate tectonics: the Midcontinent gravity high. Earth and Planetary Science Letters, **21**: 70–78

Daniels, P.A. 1982. Upper Precambrian sedimentary rocks: Oronto Group, Michigan–Wisconsin. *In* Geology and tectonics of the Lake Superior basin. *Edited by* R.J. Wold and W.J. Hinze. Geological Society of America, Memoir 156, pp. 107–133.

Davis, D.W., and Green, J.C. 1997. Geochronology of the North American Midcontinent rift in western Lake Superior and implications for its geodynamic evolution. Canadian Journal of Earth Sciences, **34**(4): 476–488.

Davis, D.W., and Paces, J.B. 1990. Time resolution of geologic events on the Keweenaw Peninsula and implications for development of the Midcontinent Rift system. Earth and Planetary Science Letters, **97**: 54–64.

Davis, D.W., and Sutcliffe, R.H. 1985. U–Pb ages from the Nipigon plate and northern Lake Superior. Geological Society of America Bulletin, **96**: 1572–1579.

Fan, J., and Kerrich, R. 1997. Geochemical characteristics of aluminum depleted and undepleted komatiites and HREE-enriched low-Ti tholeiites, western Abitibi greenstone belt: a heterogeneous mantle plume-convergent margin. Geochimica et Cosmochimica Acta, **61**: 4723–4744.

Fowler, J.H., and Kuenzi, W.D. 1978. Keweenawan turbidites in Michigan (deep borehole redbeds): a foundered basin sequence developed during evolution of a protooceanic rift system. Journal of Geophysical Research, **83**: 5833–5843.

Fralick, P.W. 1999. Paleohydraulics of chute-and-pool structures in a Paleoproterozoic fluvial sandstone. Sedimentary Geology, **125**: 129–134.

Fralick, P.W. 2003. Geochemistry of clastic sedimentary rocks: ratio techniques. *In* Geochemistry of sediments and sedimentary rocks: evolutionary considerations to mineral deposit-forming environments. *Edited by* D. Lentz. Geological Association of Canada, GEOtext 4, pp. 85–103.

Fralick, P.W., and Kronberg, B.I. 1997. Geochemical discrimination of clastic sedimentary rock sources. Sedimentary Geology, **113**: 111–124.

Franklin, J.M. 1970. Metallogeny of the Proterozoic rocks of Thunder Bay District, Ontario. Ph.D. thesis, University of Western Ontario, London, Ont.

Frey, F.A., Wise, W.S., Garcia, M.O., West, H., Kwon, S.T., and Kennedy, A. 1990. Evolution of Mauna Kea Volcano, Hawaii: petrologic and geochemical constraints on postshield volcanism. Journal of Geophysical Research, B, Solid Earth and Planets, **95**: 1271–1300.

Gibson, S.A., Thompson, R.N., and Dickin, A.P. 2000. Ferropicrites: geochemical evidence for Fe-rich streaks in upwelling mantle plumes. Earth and Planetary Science Letters, **174**: 355–374.

Giguère, J.F. 1975. Geology of St. Ignace Island and adjacent islands, District of Thunder Bay. Ontario Ministry of Natural Resources, Geological Report 118.

Green, J.C. 1977. Keweenawan plateau volcanism in the Lake Superior region. *In* Volcanic regimes of Canada. *Edited by* W.R.A. Baragar, L.C. Coleman, and J.M. Hall. Geological Association of Canada, Special Paper 16, pp. 407–422.

Green, J.C. 1981. Pre-Tertiary continental flood basalts. *In* Basaltic volcanism on the terrestrial planets. Basaltic Volcanism Study Project, Pergamon Press, Inc., New York, pp. 30–77.

Green, J.C. 1983. Geological and geochemical evidence for the nature and development of the Middle Proterozoic (Keweenawan) Midcontinental Rift of North America. Tectonophysics, **94**: 413–437.

Halls, H.C. 1972. Magnetic studies in northern Lake Superior. Canadian Journal of Earth Sciences, **9**: 1349–1367.

Halls, H.C. 1974. A paleomagnetic reversal in the Osler Volcanic Group, northern Lake Superior. Canadian Journal of Earth Sciences, **11**: 1200–1207.

Hamblin, W.K. 1961. Paleogeographic evolution of the Lake Superior region from Late Keweenawan to Late Precambrian time. Geological Society of America Bulletin, **72**: 1–18.

Hamblin, W.K. 1965. Basement control of Keweenawan and Cambrian sedimentation in the Lake Superior region. American Association of Petroleum Geologists Bulletin, **49**: 950–959.

Hanson, G.N. 1975. $^{40}Ar/^{39}Ar$ spectrum ages on Logan intrusions, a Lower Keweenawan flow and mafic dikes in northeastern Minnesota – northwestern Minnesota. Canadian Journal of Earth Sciences, **12**: 821–835.

Hart, T.R., MacDonald, C.A., Hollings, P., and Richardson, A. 2005. Proterozoic intrusive rocks of the Nipigon Embayment and Midcontinent Rift. *In* Proceedings of the 10th International Platinum Symposium, Oulu, Finland, 8–11 August 2005. *Edited by* T.O. Tormanen and T.T. Alapieti. CIM Special Vol. 54, pp. 362–364.

Heaman, L.M., and Easton, R.M. 2005. Proterozoic history of the Lake Nipigon area, Ontario: constraints from U–Pb zircon and baddeleyite dating. *In* Proceedings of the 51st Annual Meeting of the Institute on Lake Superior Geology, Nipigon, Ont. *Edited by* R.M. Easton and P. Hollings. Part 1, Program and Abstracts, Vol. 51, pp. 24–25.

Heaman, L.M., and Machado, N. 1992. Timing and origin of the Midcontinent Rift alkaline magmatism, North America: evidence from the Coldwell Complex. Contributions to Mineralogy and Petrology, **110**: 289–303.

Heggie, G.J. 2005. Whole rock geochemistry, mineral chemistry, petrology and Pt, Pd mineralization of the Seagull Intrusion, northwestern Ontario. M.Sc. thesis, Lakehead University, Thunder Bay, Ont.

Hinze, W., Allen, D., Fox, A., Sunwood, D., Woelk, T., and Green,

A. 1992. Geophysical investigations and crustal structure of the North American Midcontinent Rift system. Tectonophysics, **213**: 17–32.

Hutchinson, D.R., White, R.W., Cannon, W.F., and Schulz, K.J. 1990. Keweenaw hot spot: geophysical evidence for a 1.1 Ga mantle plume beneath the Midcontinent Rift System. Journal of Geophysical Research, **95**: 10 869 – 10 884.

Kalliokoski, J. 1982. The Jacobsville sandstone. *In* Geology and tectonics of the Lake Superior basin. *Edited by* R.J. Wold and W.J. Hinze. Geological Society of America, Memoir 156, pp. 147–156.

Klewin, K.W., and Berg, J.H. 1990. Geochemistry of the Mamainse Point volcanics, Ontario, and implications for the Keweenawan paleomagnetic record. Canadian Journal of Earth Sciences, **27**(9): 1194–1199.

Klewin, K.W., and Berg, J.H. 1991. Petrology of Keweenawan Mamainse Point lavas, Ontario: petrogenesis and continental rift evolution. Journal of Geophysical Research, **96**: 457–474.

Klewin, K., and Shirey, S.B. 1992. The igneous petrology and magmatic evolution of the Midcontinent rift system. Tectonophysics, **213**: 33–40.

Krogh, T.E., Corfu, F., Davis, D.E., Dunning, G.R., Heaman, L.M., Kamo, S.L., and Machado, N. 1987. Precise U–Pb isotopic ages of diabase dikes and mafic to ultramafic rocks using trace amounts of baddeleyite and zircon. *In* Mafic dike swarms. *Edited by* H.C. Halls and W.F. Fahrig. Geological Association of Canada, Special Paper 43, pp. 147–152.

Lightfoot, P., Sutcliffe, R., and Doherty, W. 1991. Crustal contamination identified in Keweenawan Osler Group tholeiites, Ontario: a trace element perspective. Journal of Geology, **99**: 739–760.

McDonald, B.C., and Banerjee, L. 1971. Sediments and bedforms on a braded outwash plain. Canadian Journal of Earth Sciences, **8**: 1282–1301.

McIlwaine, W.H., and Wallace, H. 1976. Geology of the Black Bay Peninsula area, District of Thunder Bay, accompanied by map 2304 (scale 1 inch to 1 mile). Ontario Division of Mines, Geological Report 133.

Merk, G.P., and Jirsa, M. 1982. Provenance and tectonic significance of the Keweenawan interflow sedimentary rocks. *In* Geology and tectonics of the Lake Superior basin. *Edited by* R.J. Wold and W.J. Hinze. Geological Society of America, Memoir 156, pp. 97–105.

Miall, A.D. 1978. Lithofacies types and vertical profile models in braided river deposits: a summary. *In* Fluvial sedimentology. *Edited by* A.D. Miall. Canadian Society of Petroleum Geologists, Memoir 5, pp. 597–604.

Nicholson, S.W., and Shirey, S.B. 1990. Midcontinent rift volcanism in the Lake Superior region: Sr, Nd, and Pb isotopic evidence for a mantle plume origin. Journal of Geophysical Research, **95**: 10 851 – 10 868.

Nicholson, S.W., Shirey, S.B., and Green, J.C. 1991. Regional Nd and Pb isotopic variations among the earliest Midcontinent Rift basalts in western Lake Superior. Geological Association of Canada – Mineralogical Association of Canada, Program with Abstracts, **16**: A90.

Nicholson, S.W., Shirey, S.B., Schulz, K.T., and Green, J.C. 1997. Rift-wide correlation of 1.1 Ga Midcontinent rift system basalts: implications for multiple mantle sources during rift development. Canadian Journal of Earth Sciences, **34**(4): 504–520.

Ojakangas, R.W., and Morey, G.B. 1982*a*. Keweenawan prevolcanic quartz sandstones and related rocks of the Lake Superior region. *In* Geology and tectonics of the Lake Superior basin. *Edited by* R.J. Wold and W.J. Hinze. Geological Society of America, Memoir 156, pp. 85–96.

Ojakangas, R.W., and Morey, G.B. 1982*b*. Keweenawan sedimentary rocks of the Lake Superior region: a summary. *In* Geology and tectonics of the Lake Superior basin. *Edited by* R.J. Wold and W.J. Hinze. Geological Society of America, Memoir 156, pp. 157–164.

Paces, J.B. 1988. Magmatic processes, evolution and mantle source characteristics contributing to the petrogenesis of Midcontinent Rift basalts: Portage Lake basalts, Keweenaw Peninsula, Michigan. Ph.D. thesis, Michigan Technological University, Houghton, Mich.

Paces, J.B., and Bell, K. 1989. Non-depleted subcontinental mantle beneath the Superior Province of the Canadian Shield: Nd–Sr isotopic and trace element evidence from Midcontinent Rift basalts. Geochimica et Cosmochimica Acta, **53**: 2023–2035.

Paces, J.B., and Miller, J.D. 1993. Precise U–Pb ages of Duluth Complex and related mafic intrusions, northeastern Minnesota: geochronological insights to physical, petrogenetic, paleomagnetic, and tectonomagnetic processes associated with the 1.1 Ga Midcontinent Rift System. Journal of Geophysical Research, B, Solid Earth and Planets, **98**: 13 997 – 14 013.

Palmer, H.C., and Davis, D.W. 1987. Paleomagnetism and U–Pb geochronology of Michipicoten Island: precise calibration of the Keweenawan polar wander tract. Precambrian Research, **37**: 157–171.

Richardson, A., and Hollings, P. 2005. Geochemical variation within the Mesoproterozoic Nipigon diabase sills. *In* Proceedings of the 51st Annual Meeting of the Institute on Lake Superior Geology, Nipigon, Ont. *Edited by* R.M. Easton and P. Hollings. Part 1, Program and Abstracts, Vol. 51, pp. 52–53.

Rogala, B., Fralick, P.W., and Metsaranta, R. 2005. Stratigraphy and sedimentology of the Mesoproterozoic Sibley Group and related igneous intrusions, northwestern Ontario. Ontario Geological Survey, Open File Report 6174.

Shirey, S.B. 1997. Re–Os isotopic compositions of Midcontinent rift system picrites: implications for plume–lithosphere interaction and enriched mantle sources. Canadian Journal of Earth Sciences, **34**(4): 489–503.

Shirey, S., Klewin, K., Berg, J., and Carlson, R. 1994. Temporal changes in the sources of flood basalts: isotopic and trace element evidence from the 1100 Ma old Keweenawan Mamainse Point Formation, Ontario, Canada. Geochimica et Cosmochimica Acta, **58**: 4475–4490.

Sun, S.S., and McDonough, W.F. 1989. Chemical and isotopic systematics of oceanic basalts: implications for mantle composition and processes. *In* Magmatism in the ocean basins. *Edited by* A.D. Saunders and M.J. Norry. Geological Society (of London), Special Publication 42, pp. 313–345.

Sutcliffe, R.H. 1987. Petrology of Middle Proterozoic diabases and picrites from Lake Nipigon, Canada. Contributions to Mineralogy and Petrology, **96**: 201–211.

Sutcliffe, R.H. 1991. Proterozoic geology of the Lake Superior region. *In* Geology of Ontario. *Edited by* P.C. Thurston, H.R. Williams, R.H. Sutcliffe, and G.M. Stott. Ontario Geological Survey, Special Vol. 4, Part 1, pp. 627–660.

Sutcliffe, R.H., and Smith, A.R. 1988. Project number 87-17. Geology of the St. Ignace Island volcanic–plutonic complex. *In* Summary of fieldwork and other activities 1988. Ontario Geological Survey, Miscellaneous Paper 141, pp. 368–371.

Tanton, T.L. 1931. Fort William and Port Arthur, and Thunder Cape map areas, Thunder Bay District, Ontario. Geological Survey of Canada, Memoir 167.

Thériault, R.D., Barnes, S.-J., and Severson, M.J. 1997. The influence of country-rock assimilation and silicate to sulfide ratios (*R* factor) on the genesis of the Dunka Road Cu–Ni–platinum-group

element deposit, Duluth Complex, Minnesota. Canadian Journal of Earth Sciences, **34**(4): 375–389.

Van Schmus, W.R. 1992. Tectonic setting of the Midcontinent Rift system. Tectonophysics, **213**: 1–15.

Van Schmus, W.R., Green, J.C., and Halls, H.C. 1982. Geochronology of Keweenawan rocks in the Lake Superior region. *In* Geology and tectonics of the Lake Superior basin. *Edited by* R.J. Wold and W.J. Hinze. Geological Society of America, Memoir 156, pp. 165–172.

Vervoort, J.D., and Green, J.C. 1997. Origin of evolved magmas in the Midcontinent rift system, northeast Minnesota: Nd-isotope evidence for melting of Archean crust. Canadian Journal of Earth Sciences, **34**(4): 521–535.

Weiblen, P.W., and Morey, G.B. 1980. Summary of the stratigraphy, petrology and structure of the Duluth Complex. American Journal of Science, **280**: 88–133.

White, R.S., and McKenzie, D.P. 1995. Mantle plumes and flood basalts. Journal of Geophysical Research, **100**: 17 543 – 17 586.

White, W.S. 1972. Keweenawan flood basalts and continental rifting. Geological Society of America, Abstracts with Programs, **4**: 732–734.

Wirth, K.R., Vervoort, J.D., and Naiman, Z.J. 1997. The Chengwatana Volcanics, Wisconsin and Minnesota: petrogenesis of the southernmost volcanic rocks exposed in the Midcontinent rift. Canadian Journal of Earth Sciences, **34**(4): 536–548.

Wolff, R.G., and Huber, N.K. 1973. The Copper Harbour Conglomerate (Middle Keweenawan) on Isle Royale, Michigan, and its regional implications. US. Geological Survey, Professional Paper 754-B.

Zartman, R.E., Nicholson, S.W., Cannon, W.F., and Morey, G.B. 1997. U–Th–Pb zircon ages of some Keweenawan Supergroup rocks from the south shore of Lake Superior. Canadian Journal of Earth Sciences, **34**(4): 549–561.

Appendix A: Summary of field descriptions for sedimentary units in the Osler Group

Simpson Island Formation, lower member

Lower conglomeratic assemblage

Sandstones of the Nipigon Bay Formation are overlain by pebble–cobble conglomerates of the Simpson Island Formation. The basal conglomerate cuts down 2 m into the Nipigon Bay Formation over a lateral distance of 15 m. This lower unit is composed of massive conglomerate. Most of the clasts are pebbles, with the largest clasts having a diameter of 20 cm. Clast lithologies consist of quartz, red siltstone, various types of unmetamorphosed volcanic rocks, gunflint cherts, and rarer metamorphosed igneous rocks of assorted types. The pebbles are subangular to subrounded, whereas the associated coarse to very coarse sandstones contain grains that are angular to subangular. The lowermost conglomerate thickens laterally and is overlain by parallel-laminated pebbly sandstones, reminiscent of a longitudinal bar with a bar tail sand wedge draping it. The draping pebbly sandstones consist of 3–20 cm thick beds. The layers have some lateral continuity but erosively cut into one another. Internally they are upper flow regime parallel laminated with pebble-rich areas. The pebble-rich areas form low-relief mounds with flat pebbles inclined in opposite directions on either side of the mounds. These are 10–15 cm across, 3 cm high, and near the base of the layer. They are reminiscent of antidune-built transverse ribs. There are also features that resemble shoot and pool structures. The tops of some layers are cross-stratified. The aforementioned sandstones are interbedded with massive pebbly sandstones that average 60 cm thick. The entire assemblage is 3 m thick and overlain by trough cross-stratified sandstone lenses.

Middle cross-stratified sandstone assemblage

The middle cross-stratified sandstone assemblage is composed of medium-grained sandstones with scattered pebbles, pebble stringers, and pebbly lenses (pebbly sandstone lenses). The pebble stringers and pebbly sandstones form lags at the base of trough-shaped scours. Pebbles are rounded to subrounded, with varied lithologies similar to those of the underlying conglomerates. The lenses average 15 cm by 100 cm, and trough cross-stratification is abundant. Paleocurrent direction is 300°.

Upper conglomeratic assemblage

The trough cross-stratified sandstones are sharply overlain by massive conglomerates of the upper conglomeratic assemblage. These conglomerate layers are up to 2 m thick and contain lenses of trough cross-stratified, medium-grained sandstone. In places, they are laterally transitional into wedges of medium-scale planar cross-stratified, medium-grained sandstones. The conglomerates are interbedded with trough cross-stratified sandstone layers up to 1 m thick. Clast lithologies in the conglomerates are varied but are dominated by quartz, unmetamorphosed basalt, and granitic compositions. The matrix in the conglomerates consists of grain sizes from pebbles to coarse sand, whereas the thicker sandstone beds are composed of medium-grained sand. The coarse-grained sand in the matrix contains a very large proportion of lithic fragments. Paleocurrent directions are as follows: 250°, 265°, 270°, 252°, 277°, 230°, 252°, 307°, 143°, and 040°.

Upper cross-stratified sandstone

The upper cross-stratified sandstone overlies the conglomeratic assemblage and is composed of poorly sorted, medium-grained sandstones with coarse and very coarse grains floating in them. The sandstones are pebbly in places and contain pebble stringers and shale poker chip intraformational conglomeratic horizons. The assemblage is composed of trough cross-stratified units up to 100 cm thick, averaging 50 cm thick. Paleocurrent directions are as follows: 130°, 290°, 265°, 000°, 295°, 285°, 310°, 315°, 295°, 345°, 000°, and 195°.

Simpson Island Formation, upper member

Section 5: lower sheet sandstone

Immediately above the volcanic rocks is a series of conglomerates and sandstones. The exposed conglomerate is 1.5 m thick and composed of laterally continuous sheets of pebble conglomerate and pebbly sandstone 10–30 cm thick. The matrix material is siltier and less well sorted than conglomerates higher in the outcrop interval. Clast orientations in some layers are chaotic. The conglomerate is overlain by 5 m of sharp-sided, laterally continuous, upper flow regime, parallel-laminated sandstones and pebbly sandstones. Scattered

clasts in the sandstones are rounded, but to a lesser degree than overlying clasts. Maximum clast size is 10 cm.

Section 5: upper conglomeratic unit

The upper conglomeratic unit is dominated by rounded to very well-rounded, cobble–pebble conglomerates with a well-sorted, medium-grained sand matrix. The sorting of the clasts is also quite good. Layering within the conglomerates is denoted by changes in clast size, but these are not very pronounced. Most of the clasts are derived from the Sibley Group, with these dominated by cream-coloured, quartz-rich sandstones similar to those in the Nipigon Bay Formation, upon which this unit rests. Unmetamorphosed mafic volcanic clasts are also fairly prevalent (up to 30% in places), and there are a few granite cobbles. The largest clast is 30 cm. The conglomerate contains medium-grained sandstone lenses about 1 m apart vertically. Some of the lenses were produced by uneven erosion of a once more continuous sand layer, whereas others are true lenses. The larger, erosion-formed lenses have a maximum size of 30 cm by 600 cm. The smaller true lenses have a maximum size of 10 cm by 70 cm. All are cross-stratified (mostly trough), some with pebbles and cobbles on cross-stratification surfaces. One cross-stratified sandstone was laterally transitional to upper flow regime, parallel-laminated sand over a 10 m interval, and then it turned into a series of dipping sand and gravel layers. Paleocurrent directions are as follows: 160°, 280°, 235°, 275°, 265°, 280°, 305°, 260°, and 265°.

Section 6

The following description of section 6 is from bottom to top of the outcrop. (1) Basalt flows, 3 m covered, 30 cm of very mafic, medium-grained sandstone. This looks like the basalt but has abundant rounded quartz grains, and it may be regolith. (2) Thirty centimetres of matrix-supported, pebble conglomerate with red sandstone, basalt, and quartz clasts. Pebbles are randomly orientated, and the matrix is sandy but poorly sorted. (3) Six metres of wave ripple laminated, very fine grained red sandstone. Layers average 1 cm thick and have millimetre-scale shale drapes. Draping foresets are abundant in the oscillation ripples. Some 2–3 cm thick, fine-grained sandstones are present with upper flow regime parallel lamination and parting lineation. These are overlain by small-scale hummocky cross-stratification, and this in turn is overlain by oscillation rippled very fine grained sandstones. These successions are up to 20 cm thick. Mud chips are also present in some of the sands. The 6 m thick succession becomes coarser upwards, and the layers become thicker upwards. Medium-grained sandstones dominate in the upper couple of metres, with only widely spaced shale partings. Paleocurrent directions are 302° and 280°. (4) Eight metres covered. (5) Seven metres of interlayered pebbly sandstone, medium-grained sandstone, matrix-supported conglomerate, and limited pockets of clast-supported conglomerate. Pebble bands are commonly aligned at various angles following erosion surfaces and dipping laminae. Medium- and large-scale festoon (trough) cross-stratification dominates. This resembles portions of the Van Horn Sandstone. The larger pebbles are subrounded, the smaller ones subangular, and the sand is angular. The sediment is immature. Clasts consist of volcanic rocks, dominated by unmetamorphosed basalt, quartz, granite, and minor amounts of Sibley lithologies. Paleocurrent directions are 010°, 245°, 055°, 005°, 200°, 175°, 055°, 060°, 280°, and 255°. (6) Four metres of interlayered lenses of trough cross-stratified conglomerates and sandstones.

Puff Island assemblage

The following description of the Puff Island assemblage is from bottom to top of the outcrop. (1) One and a half metres of pebbly, coarse-grained sandstones organized in laterally continuous layers 1–6 cm thick and forming packages up to 60 cm thick. These are scoured into by pebble–cobble conglomeratic lenses. Caliche layers are present. (2) Four metres of massive, disorganized bedded, boulder–cobble conglomerate. No sedimentary structures, imbrication, or layering of any kind. Clasts are up to 1.5 m in diameter. The matrix is very poorly sorted but mostly sand sized. All observed clasts are of lithologies present in the rift assemblage. Feldspar porphyries are common, though it is difficult to distinguish felsic and mafic clasts because everything has weathered red. Mafic clasts form a substantial portion of the clasts. (3) Two metres of interstratified granule to pebbly sandstones and pebble to cobble conglomerates. The sandstone beds are very wispy and no more than 15 cm thick. Bed contacts are indistinct but are present. All units are irregular, lensey, and interfingering. Larger clasts are mostly subrounded. Granules and sand are angular to subangular. Hematite is abundant. A boulder at the top of the succession sticks into the next sequence and has a crescent scour and sand shadow developed, giving a flow direction of 140°. (4) Two metres of strata similar to those of the basal unit. Here the caliche layers are ~2 cm thick and 5–10 cm apart. (5) Seven metres of interlayered lensey, cobble–pebble conglomerate and coarse-grained pebbly sandstone. The basal contact is a sharp scoured horizon that irregularly cuts down into the underlying unit. Very large-scale trough cross-stratification fills this sour and indicates the current was going toward 130°. Bed contacts are indistinct and irregular. The upper third of the unit is dominated by sandstone lenses up to 1 m by 5 m. There are also some lenses of conglomerate, and siltstone lenses begin to appear. (6) Eight metres of trough cross-stratified sandstone with pebble and cobble mounds scattered throughout. The sandstones are well laminated with upper flow regime parallel lamination and trough cross-stratification dominating. Average flow for this unit is towards 135°. The sandstone layers are not really lenses because they are somewhat laterally continuous, but they do cut down into one another and abut abruptly against cobble hills. There are some pebble conglomerate layers, and a few are nicely graded from golfball-sized clasts to medium-grained sandstone over 25 cm vertically. The cobble and pebble mounds are generally one or two cobbles in height and 1 m long. Basalt overlies this assemblage.